Report No. UT-04.09

ANALYTICAL MODELING OF MSE WALL AT I-15 AND 3600 SOUTH

Prepared For:

Utah Department of Transportation
Research and Development Division

Submitted By:

Utah State University
Department of Civil & Environmental Engineering
Logan, Utah

Authored By:

Dr. James A. Bay, Associate Professor
Dr. Loren R. Anderson, Professor
Aaron S. Budge
Chatchai Eurfur

November 2004

UDOT RESEARCH & DEVELOPMENT REPORT ABSTRACT

1. Report No. UT-04.09	**2. Government Accession No.**	**3. Recipient's Catalog No.**
4. Title and Subtitle ANALYTICAL MODELING OF MSE WALL AT I-15 AND 3600 SOUTH	**5. Report Date** November 2004 **6. Performing Organization Code**	
7. Author(s) Bay, James A. Anderson, Loren R. Budge, Aaron S. Eurfur, Chatchai	**8. Performing Organization Report No.**	
9. Performing Organization Name and Address Department of Civil and Environmental Engineering Utah State University Logan, UT 84322-4110	**10. Work Unit No.** **11. Contract No.** 019118	
12. Sponsoring Agency Name and Address Utah Department of Transportation Research Division 4501 South 2700 West Salt Lake City, Utah	**13. Type of Report and Period Covered** Research 1999 - 2004 **14. Sponsoring Agency Code** 81SR0123 / PIC No. UT00.503	
15. Supplementary Notes UDOT Research Project Managers - Clifton Farnsworth and Blaine Leonard		

16. Abstract

This report is the culmination of extensive research into the behavior of an MSE wall at I-15 and 3600 South in Salt Lake City, Utah. The wall is about 30 ft tall and is constructed on a compressible, soft clay foundation. Earlier work has included extensive instrumentation and monitoring of stresses and deformations in the wall and its foundation, a study of the effects of drilling and sampling method on disturbance of samples, and extensive laboratory testing to determine strength and deformation properties of soils at the site. All of this work has been used to develop and calibrate an analytical model of the MSE wall. This report describes this analytical model.

17. Key Words mechanically stabilized earth wall, MSE wall, numerical model, stability analysis		**18. Distribution Statement**	
19. Security Classification (of this report) N/A	**20. Security Classification (of this page)** N/A	**21. No. of Pages** 66	**22. Price**

DISCLAIMER

The authors alone are responsible for the preparation and accuracy of the information, data, analysis, discussions, recommendations, and conclusions presented herein. The contents do not necessarily reflect the views, opinions, endorsements, or policies of the Utah Department of Transportation (UDOT) or the US Department of Transportation (USDOT). The Utah Department of Transportation makes no representation or warranty of any kind, and assumes no liability therefore.

Report No. UT-04.09

ANALYTICAL MODELING OF MSE WALL AT I-15 AND 3600 SOUTH

Prepared For:

Utah Department of Transportation
Research and Development Division
Salt Lake City, Utah

Submitted By:

Utah State University
Department of Civil & Environmental Engineering
Logan, Utah

Authored By:

Dr. James A. Bay, Associate Professor
Dr. Loren R. Anderson, Professor
Aaron S. Budge
Chatchai Eurfur

November 2004

EXECUTIVE SUMMARY

This report presents the results of a two-dimensional finite element model of the mechanically stabilized earth (MSE) wall located on I-15 at 3600 South in Salt Lake City, Utah. The model was created and calibrated using data collected at the construction site during and after construction of the wall (see Report No. UT-03.11 - "Instrumentation and Installation Scheme of a Mechanically Stabilized Earth Wall on I-15 With Results of Wall and Foundation Behavior"). The model also took into account the results of extensive laboratory testing on samples collected at the site (see Report No. UT-03.13 - "Evaluation of SHANSEP Parameters for Soft Bonneville Clays", and Report No. UT-03.14 - "Factors Affecting Sample Disturbance in Bonneville Clays"). Such a model is a powerful tool in understanding the behavior of a tall MSE wall on a compressible foundation.

This analytical model includes a number of soil models to represent the range of soils in the foundation of the wall, as well as additional soil models to represent the fill material used for the original I-15 embankment and the new material used to construct the MSE wall. Trench drains, with adjusted soil permeabilities, were used to represent the prefabricated vertical drains (PVDs) used at the site. The bar mat reinforcement used to construct the wall was also modeled, with special consideration regarding the effects of soil-reinforcement interaction.

The analytical model was calibrated to match the measured long term horizontal and vertical deflections at the wall site. Once this was accomplished, the effective permeability of the foundation soil was adjusted and the construction sequence approximated in order to match the time settlement behavior of the wall. When the model was considered to accurately represent the MSE wall for both the long- and short-term behavior, a stability analysis was performed at various stages of construction to observe the external stability of the wall throughout the construction process and in the years following construction. For the model following the staged construction of the

wall, the factor or safety for the original embankment was 2.03. This value increased slightly as the wall was built, since initially the wall acted as a berm, forcing the failure surface up the embankment. However, once the wall was approximately halfway constructed, the failure surface was forced into the foundation material, and the factor of safety decreased to a minimum value of 1.47 at the application of the surcharge load, then increased with consolidation to a value of 1.69 for the long term factor of safety for the MSE wall at final grade. A minimum factor of safety of 1.16 was calculated for instantaneous construction of the wall, which increased with consolidation to a value nearly identical to the long-term value obtained from the staged construction.

As determined during the global stability analysis, the predicted failure surface has a V-shape, with total movement being downward and away from the original embankment in the backfill material and the foundation material beneath the wall backfill, and with total movement being upward and away from the wall in the foundation material outside the wall footprint. It is noteworthy that such a failure surface might not be predicted using some automated traditional slope stability analyses, where a circular or spiral failure surface is typically used to compute a factor of safety. Slope stability software packages that allow for manually specified failure surface could better approximate such a failure mechanism, assuming such a surface was anticipated by the user. For this case, it appears that a traditional slope stability approach might not be conservative, especially if the stability analysis required a circular or spiral failure surface. This is a key reason for using a finite element program to perform slope stability (or other stability) evaluations instead of the more traditional software packages that may be limited to circular or spiral failure surfaces.

The effects of pore pressure dissipation during construction can be evaluated, and were taken into account during the stability analyses and in calibrating the time-settlement behavior. The effects of excess pore pressure were significant. Substantial excess pore pressures developed during the construction process, and dissipated with time. However, the pore pressures that developed were much less than those that would occur if an immediate, undrained construction had occurred. Thus, an undrained strength

approach would be quite conservative, while a drained strength approach would be unconservative. Using a soil model that accounts for the generation and dissipation of pore pressures and accounts for those excess pore pressures in performing stability analyses is of the utmost importance.

The ability to model the interaction between the soil and the reinforcement is somewhat limited, due to the limitations in the Plaxis software. However, a model was developed that overestimates the tension in the reinforcement in the lower portion of the wall while underestimating the tension in the upper portion of the wall. With this limited and simplified model of the soil-reinforcement interaction, an analysis of some additional failure modes was performed. The external modes of overturning and sliding were investigated, while internal modes relating to pull-out failure and tensile failure of the reinforcement were not considered. These analyses resulted in a factor of safety for sliding of approximately 1.9 and a factor of safety for overturning of approximately 2.1.

TABLE OF CONTENTS

Page

Page

LIST OF TABLES

LIST OF FIGURES

1.0 Introduction

This report is the culmination of extensive research into the behavior of MSE Wall R-346-1C located at I-15 and 3600 South in Salt Lake City, Utah. The wall is along the west side of the reconstructed I-15 corridor, is about 30 ft tall, and is constructed on a compressible, soft clay foundation. Earlier work has included extensive instrumentation and monitoring of stresses and deformations in the wall and its foundation (see Report No. UT-03.11 - "Instrumentation and Installation Scheme of a Mechanically Stabilized Earth Wall on I-15 With Results of Wall and Foundation Behavior"), a study of the effects of drilling and sampling method on disturbance of samples (see Report No. UT-03.14 - "Factors Affecting Sample Disturbance in Bonneville Clays"), and extensive laboratory testing to determine strength and deformation properties of soils at the site (see Report No. UT-03.13 - "Evaluation of SHANSEP Parameters for Soft Bonneville Clays"). These reports should be consulted for a complete understanding of the site conditions, wall characteristics, and general background information. All of this work has been used to develop and calibrate an analytical model of the MSE wall. This report describes this analytical model.

The analytical model of this wall is a valuable and powerful tool to understand the behavior of tall MSE walls on compressible foundations. Using this model, the effects of pore pressure dissipation during construction can be evaluated. This allows for accurate evaluation of the stability of the embankment during construction and long-term for any construction sequence. The model can be used to evaluate soil reinforcement interaction and to evaluate different reinforcement configurations.

This report contains discussions of the soil model that was developed for Bonneville clay, a comparison between measured and calculated deformations in the wall foundation, the time-settlement behavior of the wall, stability evaluations, and soil-reinforcement interactions.

2.0 Soil Model for Bonneville Clay

One of the critical components of a model for the MSE wall is an appropriate constitutive model for the soil. A constitutive soil model must properly represent the soil's shear strength, dilative behavior, compressibility, and time-dependent behavior. Most of the deformations that occurred at the MSE wall at I-15 and 3600 South occurred in the soft Bonneville clays underlying the site. At this location, the soft, compressible Bonneville clays extend from a desiccated crust at the original ground surface to a depth of about 25 ft, with stiffer silts and clays beyond that depth. Therefore, the critical soil model for this site is the Bonneville clay model. Values of parameters used to model the soft Bonneville clay were obtained from a combination of laboratory tests on undisturbed soil specimens and matching analytical model outputs to field measurements.

2.1 The Hardening Soil Model

The soil model used in this study is the Plaxis hardening soil model (Plaxis, 2001). This effective stress model accounts for the effects of confinement and stress history on the soil moduli. It uses a hyperbolic stress-strain relationship for shear deformations. Ultimate shear strengths are characterized using a Mohr-Coulomb failure envelope. It utilizes the associated flow rule to predict plastic deformations, and a dilation angle to predict the volume change associated with plastic deformations.

The hardening soil model is probably the most comprehensive soil model available today in commercial modeling software. However, it has some deficiencies. The shear strength of soil is partially dependent on the soil's stress history. This cannot be modeled using a Mohr-Coulomb strength envelope. This is especially a problem for soils that are initially over-consolidated, but loaded beyond their maximum past pressure. This weakness can be partially overcome by using an appropriate failure envelope for the range of stresses the soil will experience.

Real soils exhibit dilative (or contractive) behavior at intermediate strain levels. The hardening soil model does not induce dilative behavior until there are plastic strains in the soil. This means that pore pressures are not induced in soils during undrained

loading until the soil is at failure. This leads to small errors in predicting undrained strength in dilative soils, but can lead to large over-predictions of undrained shear strength in contractive soils. One work-around for this problem is to use lower strength parameters when modeling the undrained strength of contractive soils.

Time dependent consolidation in soil is often divided into primary and secondary consolidation. The time rate of settlement due to primary consolidation is inversely proportional to the soil modulus and permeability, and proportional to the square of the length of the drainage path. The rate of secondary consolidation is controlled by the viscous properties of the soil. The hardening soil model does an excellent job of modeling primary consolidation, but does not account for any secondary consolidation.

Table 1 shows the parameters used in the Plaxis hardening soil model. The following equation is used to determine the modulus values as a function of confining pressure, σ'.

Table 1 Plaxis Hardening Soil Parameters

Hardening Soil Parameter	Units	Description
γ	lb/ft^3	Total unit weight
k_x	ft/day	Horizontal permeability
k_y	ft/day	Vertical permeability
ϕ'	degrees	Effective friction angle
c'	lb/ft^2	Effective cohesion
ψ	degrees	Dilation angle
E_{50}^{ref}	lb/ft^2	Reference Young's modulus
E_{oed}^{ref}	lb/ft^2	Reference constrained modulus
E_{ur}^{ref}	lb/ft^2	Reference unload/reload modulus
ν_{ur}		Unload/reload Poisson's ratio
p_{ref}	lb/ft^2	Reference stress
m		Stress exponent

$$E = E^{ref}\left(\frac{\sigma'}{p_{ref}}\right)^{m} \quad (1)$$

Where E is E_{50}, E_{oed}, or E_{ur},

and E^{ref} is E_{50}^{ref}, E_{oed}^{ref}, or, E_{ur}^{ref},

σ' is effective vertical stress, and

$m \approx 1.0$ for clays, and $m \approx 0.5$ for granular soils.

2.2 Laboratory Consolidation Measurements

Initial estimates of consolidation parameters for the foundation soils at the site were obtained from constant rate of strain (CRS) consolidation tests performed on undisturbed soil samples obtained from the site. Results from all of these consolidation tests are presented in Report No. UT-03.14, "Factors Affecting Sample Disturbance in Bonneville Clays," (Bay et.al, 2003). Figure 1a. is a consolidation curve from a typical CRS test on one of the more compressible clays. The hardening soil model uses a stress dependent modulus rather than a consolidation coefficient to model the consolidation behavior, therefore, the modulus versus effective stress is plotted in Figure 1b. In Figure 1b the virgin loading is represented by the low, linearly increasing modulus values. The higher modulus values represent the reload and unload behavior. Figure 2 shows the consolidation and modulus plots from a typical soil exhibiting lower compressibility.

Tables 2, 3, 4, and 5 contain summaries of all of the consolidation results from samples obtained from the four boreholes at the site. The average E_{oed}^{ref} for the top 16 ft at the site is 26,900 psf, and for 16-36 ft is 30,800 psf.

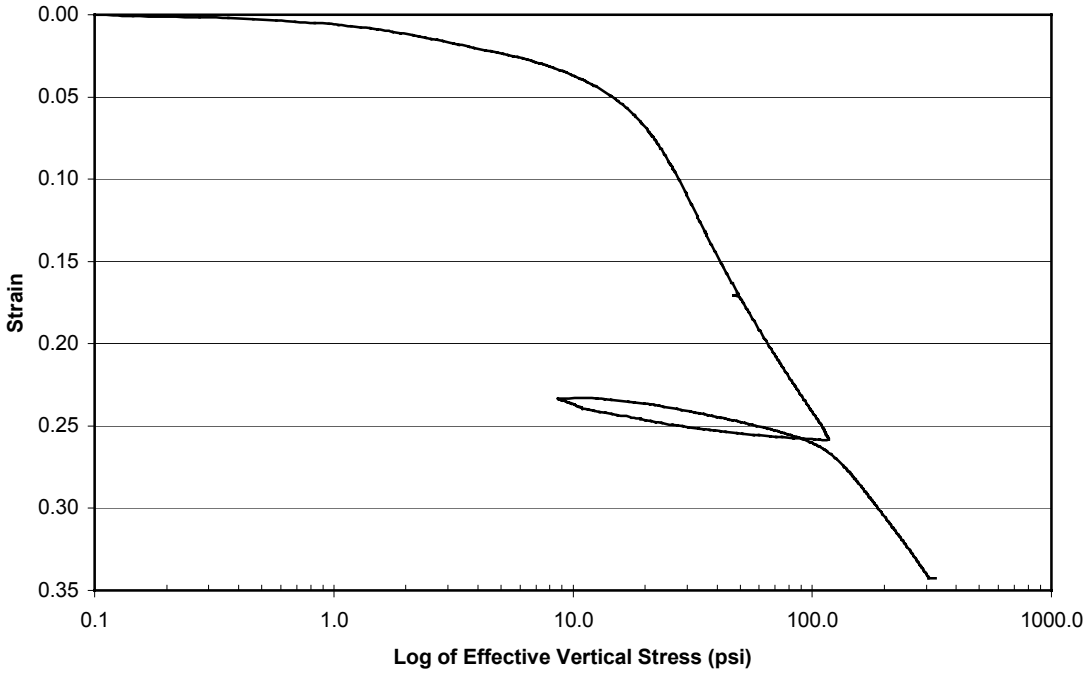

a) Consolidation Curve

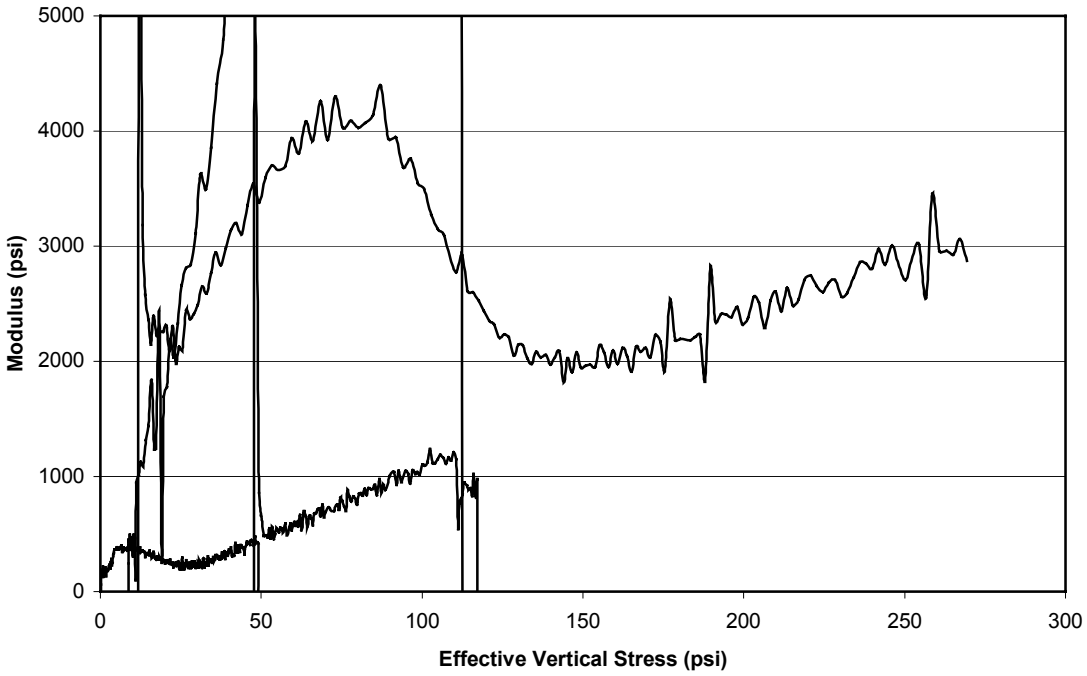

b) Modulus Curve

Figure 1 Consolidation and Modulus Curve from Boring HF-2 at 17-19 ft

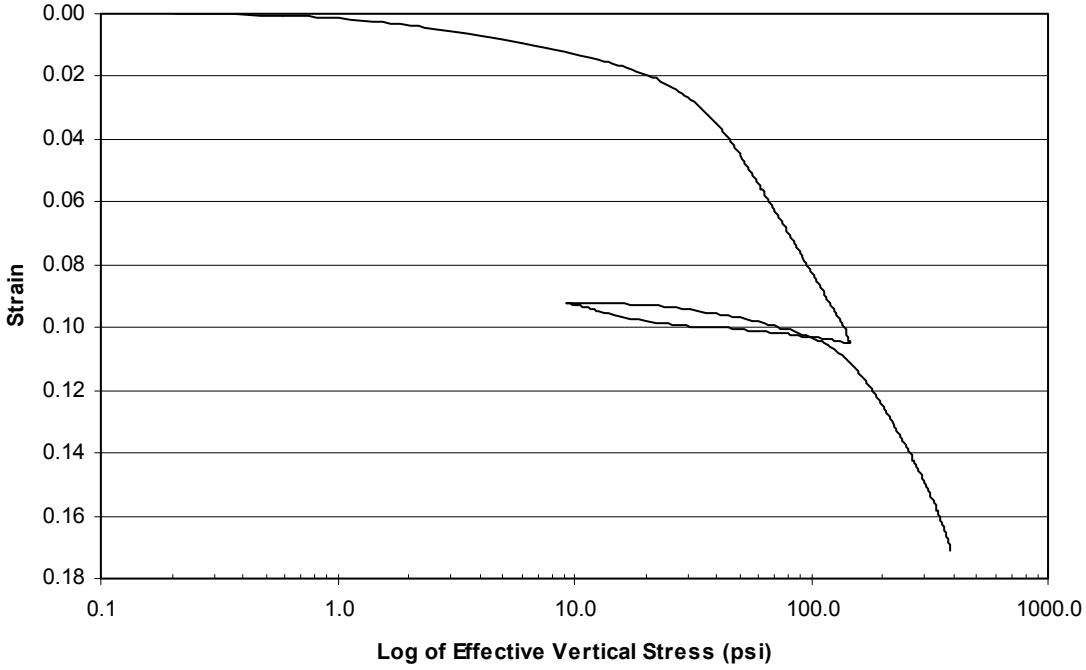

a) Consolidation Curve

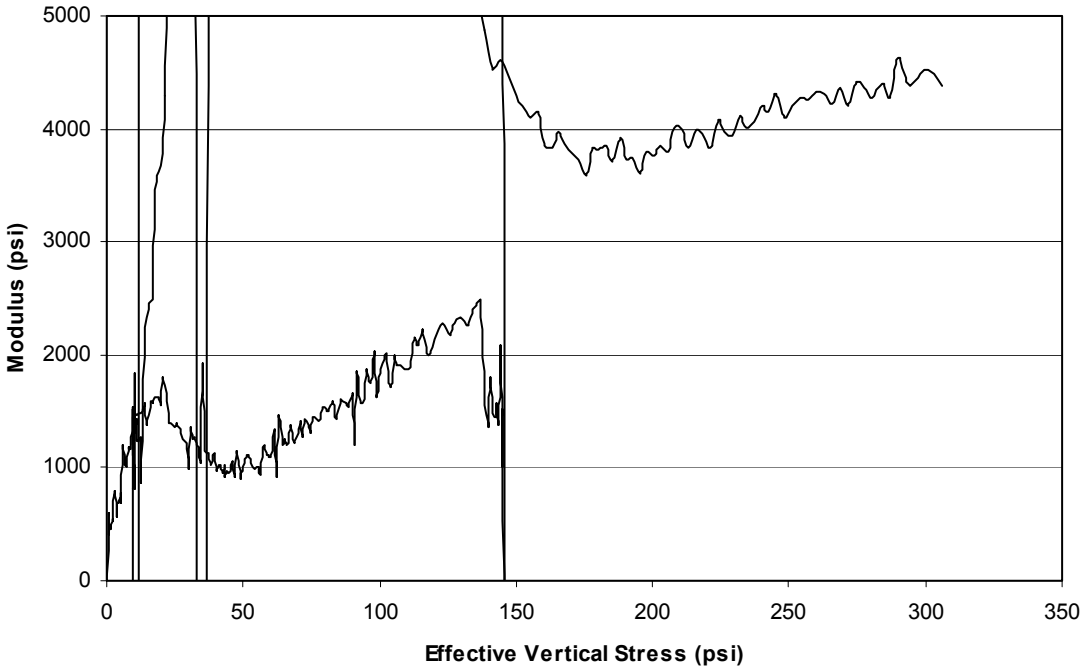

b) Modulus Curve

Figure 2 Consolidation and Modulus Curves from Boring RF-4 at 24.5-26.5 ft

Table 2 Results of CRS Consolidation Test on Soil Samples from Borehole HS-1

Depth from Surface (ft)	σ'_{vo} (psf)	σ'_{p} (psf)	E^{ref}_{oed} (psf)	$C_{c,\varepsilon}$	W_n %	PL %	LL %	% Fines	Grain size %<2μm
9.5-11.5	1080			0.135		19	32		31
12-14	1440	3312	25474	0.134		18	27		38
14.5-16.5	1555	5616	28606	0.162	31.0	23	34	99	35
17-19	1699	3456	19001	0.500	58.0	26	36	97	35
19.5-21.5	1786								
22-24	1958	4320	30485	0.139	36.4	23	32		33
24.5-26.5	2074	4464	36122	0.129	26.4	18	22	82	20
27-29	2261	4752	40925	0.112				86	19
29.5-31.5									
32-34									
34.5-36.5	2750							74	23

Table 3 Results of CRS Consolidation Test on Soil Samples from Borehole HF-2

Depth from Surface (ft)	σ'_{vo} (psf)	σ'_{p} (psf)	E^{ref}_{oed} (psf)	$C_{c,\varepsilon}$	W_n %	PL %	LL %	% Fines	Grain size %<2μm
9.5-11.5	1080	7632	24012	0.156	30.3	22	32	99	40
12-14	1440	4320	27979	0.159	33.2	22	30	98	20
14.5-16.5	1555	5040	30067	0.132	27.8	19	31	99	30
17-19	1699	2880	25056	0.269	48.7	24	37	98	38
19.5-21.5									
22-24									
24.5-26.5									
27-29									
29.5-31.5									
32-34									
34.5-36.5									

Table 4 Results of CRS Consolidation Test on Soil Samples from Borehole RS-3

Depth from Surface (ft)	σ'_{vo} (psf)	σ'_{p} (psf)	E^{ref}_{oed} (psf)	$C_{c,\varepsilon}$	W_n %	PL %	LL %	% Fines	Grain size %<2μm
9.5-11.5	1080								
12-14	1440	5328	28606	0.138	33.4	23	32	99	38
14.5-16.5	1555	6192	28606	0.170	32.6	23	33	99	30
17-19	1699	3168	25056	0.419	67.0			94	34
19.5-21.5	1786								
22-24	1958								
24.5-26.5	2074								
27-29	2261								
29.5-31.5									
32-34									
34.5-36.5	2750				21.3	19	23	89	32

Table 5 Results of CRS Consolidation Test on Soil Samples from Borehole RF-4

Depth from Surface (ft)	σ'_{vo} (psf)	σ'_{p} (psf)	E^{ref}_{oed} (psf)	$C_{c,\varepsilon}$	W_n %	PL %	LL %	% Fines	Grain size %<2μm
9.5-11.5	1080								
12-14	1440	6480	26309	0.136					
14.5-16.5	1555	7920	22133	0.129	28.3	24	32	98	40
17-19	1699	4032	27144	0.490	58.4	23	47	99	37
19.5-21.5	1786								
22-24	1958	3024	40507	0.093	32.3	18	25	77	30
24.5-26.5	2074	5040	32573	0.126	27.1	17	26	94	39
27-29	2261								
29.5-31.5									
32-34									
34.5-36.5	2750								

2.3 Maximum Past Effective Vertical Stress

Another important parameter in predicting consolidation behavior is the maximum past effective vertical stress. These values were also determined from CRS testing, and are tabulated in Table 2 through Table 5. The in situ effective vertical stress and the measured maximum past effective vertical stress are plotted in Figure 3. As is usually the case, there is considerable scatter in the maximum past effective vertical stress values. The site has a desiccated surface layer with high maximum past pressure, and below the desiccated layer the maximum past pressure roughly parallels the in situ effective vertical stress. The maximum past effective vertical stress used in the Plaxis model is also plotted in Figure 3.

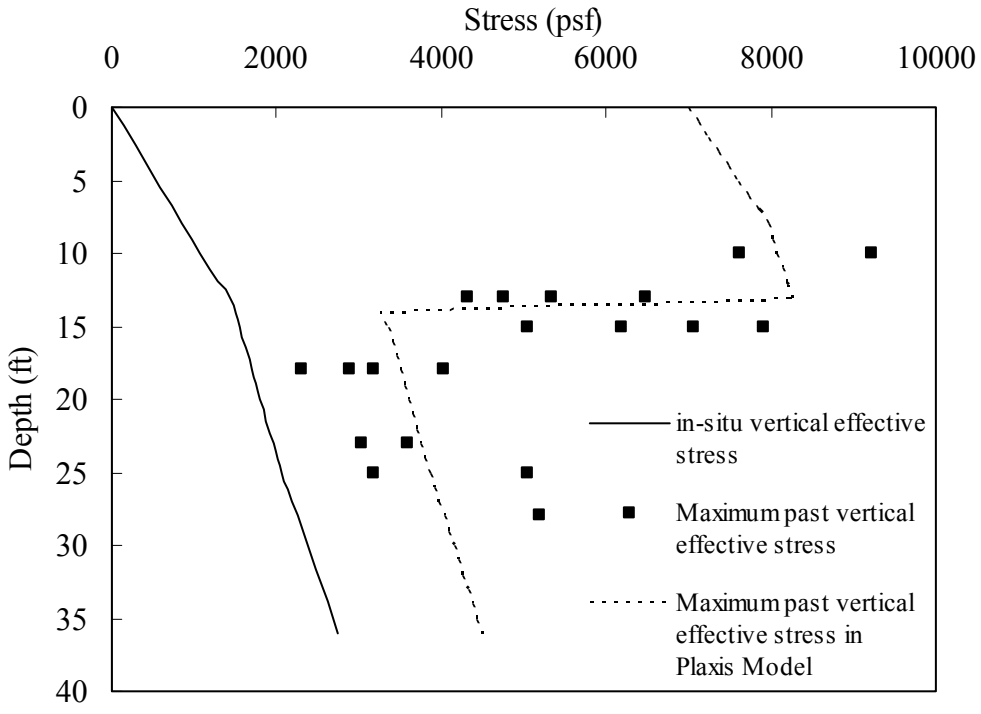

Figure 3 In Situ and Maximum Past Effective Vertical Stress at MSE Wall Site

2.4 Shear Strength Parameters

Effective shear strength parameters for the hardening soil model were obtained from $\overline{CK_0U}$ triaxial compression tests. A typical stress-strain plot from one of these tests is presented in Figure 4. Tabulated strength parameters from these tests are presented in Table 6.

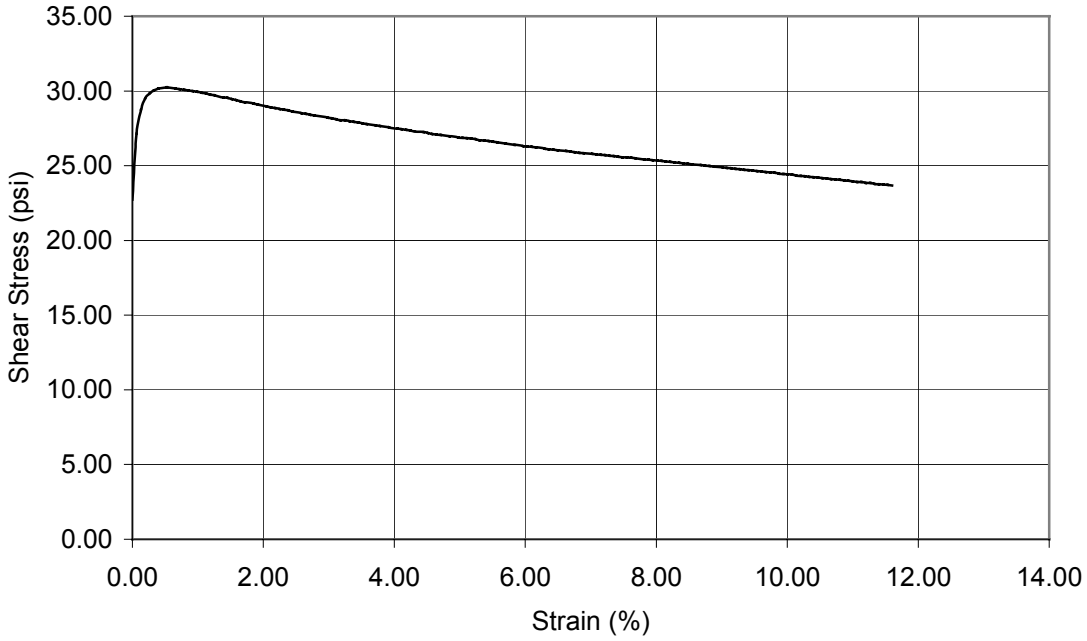

Figure 4 Shear Stress versus Strain for the 4.0 x σ'_{v0} Normally Consolidated Specimen from Boring HF-2, Depth of 18.6 ft

Table 6 Results of $\overline{CK_0U}$ Triaxial Compression Testing of Samples from 17-19 ft Depth.

Boring	σ'_{v0} (psi)	σ'_{vm} (psi)	OCR	A_f	S_u/σ'_{vm}	ϕ' (deg)*
HS-1	36	36	1.0	1.55	0.317	26.99
RS-3	60	60	1.0	1.58	0.326	27.08
HF-2	96	96	1.0	1.45	0.315	26.36
RF-4	30	60	2.0	0.36	0.595	-
RF-4	15	60	4.0	0.13	0.989	-
RF-4	10	60	6.0	0.04	1.398	-

* assuming c'=0.

One of the strengths of the hardening soil model is that it uses effective strength parameters and a pore pressure model to determine the undrained behavior of a soil model. These clays, like most clays, have an effective cohesion of zero when the clay is normally consolidated. At over consolidation ratios greater than 1 the clays will have some effective cohesion and a lower effective friction angle. Because the hardening soil model cannot account for the effect of stress history on shear strength, it was decided to use the normally consolidated strength parameters in the model. This assumption is justified because most of the foundation soils are normally consolidated after being consolidated by the embankment, and the assumption is somewhat conservative for soils that are not normally consolidated.

Modeling the undrained behavior of the embankment requires an accurate pore pressure model for the foundation. Pore pressures are generated from consolidation behavior of the embankment, and from dilation (or contraction) of the soils during shear. The hardening soil model does a very good job of model consolidation and pore pressures during consolidation. Unfortunately, the hardening soil dilation model does not accurately reflect the behavior of real contractive soils. Values of Skempton's pore pressure coefficient (A_f) shown in Table 6 describe the contractive and dilative behavior of a soil. Positive values of A_f greater than about 1.0 indicate a highly contractive soil. Values of A_f less than 0.33 indicate a dilative soil. Normally consolidated clay usually behaves as a contractive soil, and the soil should become less contractive and more dilative as the OCR increases. In Table 6 it can be seen that, in its normally consolidated state, Bonneville clay is highly contractive. The errors due to problems modeling the dilative (or contractive) behavior of the soil are probably quite low because almost all of the generated pore pressures are from consolidation, and because the soils drain quite rapidly (as will be shown later) making the undrained behavior less critical.

2.5 Soil Permeability

The time-settlement behavior and pore pressure dissipation are functions of the soil modulus, permeability and the length of the drainage paths. Prefabricated vertical drains (PVD's) were used to decrease the lengths of drainage paths and accelerate the

foundation consolidation. Flow into a PVD is a three-dimensional problem, but Plaxis is limited to two-dimensional problems. To work around this limitation trench drains were used in the Plaxis model to simulate the PVD's. Closely spaced drains were not practical for efficient calculations, so widely spaced trench drains were utilized. In order to compensate for the large spacings between drains, higher soil permeabilities were used. An iterative procedure was used to adjust the permeability until the model time-settlement accurately matched the measured time settlement. Therefore, permeabilities used in the model do not accurately represent the actual permeability of soil at the site, but rather the combination of permeability and drain spacing simulates the actual behavior at the site with PVD's.

2.6 Hardening Soil Parameters used in Plaxis Model

Initial estimates of parameters were arrived at from laboratory tests. Then these values were adjusted based upon comparisons between analytical model outputs and measured deflections at the site presented in Report No. UT-03.11 "Instrumentation and Installation Scheme of a MSE Wall on I-15 with Results of Wall and Foundation Behavior," (Bay, et.al, 2003). After numerous iterations a calibrated wall model was determined. Table 7 contains the values of parameters in this calibrated model.

The unit weight (γ) for each of the soil layers can be obtained from field specimens subjected to consolidation or triaxial tests.

The vertical permeability (k_y) can be approximated from careful consolidation tests. The horizontal permeability (k_x) can be corrected for such things as drainage path length, soil anisotropy, smear zones around drains, etc. Initially, for this model, attempts were made to approximate the horizontal permeability as five times the vertical permeability. However, it was determined that this correction made only a minimal difference, since the consolidation would be controlled by the vertical permeability of the deeper layers and not the horizontal permeability of layers where the PVDs were present.

The effective friction angle and cohesion of the various soil layers were determined from triaxial tests on soil specimens. The angle of dilation (ψ) was assumed

to be zero for this model, making the soil neither contractive nor dilative. Even though the Bonneville clay is quite contractive when normally consolidated, it was assumed that nearly all of the generated pore pressures were from consolidation rather than contraction due to shear.

Soil moduli (E_{oed}) were determined from consolidation tests. Deformations due to consolidation were much greater than deformations due to shear. Therefore, E_{50} (which expresses the shear stiffness) was assumed to be equal to E_{oed}. The unload-reload modulus was assumed to be 10 times E_{50} and an unload-reload Poisson's ratio of 0.2 was assumed. Little deformation occurred due to unload-reload, and these are reasonable approximations for most clays.

The p_{ref} value is a reference pressure used to adjust the moduli of the soil as a function of the vertical stress, as given by the hardening soil model found in Plaxis. For this project, a reference stress of 2088 psf (100 kPa) was used.

Lastly, the m value is the power for stress-level dependency of stiffness. For clays, a value of 1.0 is appropriate. For silts and sands, a value of 0.5 is appropriate.

Table 7a Hardening Soil Parameters For Calibrated Wall Model (Foundation Material)

Hardening Soil Parameters	Units	Medium Stiff Surface Clay	Soft Clay	Stiff Sandy Silt	Very Stiff Sandy Clay
γ	lb/ft^3	119.2	113	120	120
k_x	ft/day	2.5 E -03	2.5 E -03	2.5 E -03	2.5 E -03
k_y	ft/day	2.5 E -03	2.5 E -03	2.5 E -03	2.5 E -03
ϕ'	degrees	22	27	30	27
c'	lb/ft^2	750	1	750	100
ψ	degrees	0	0	0	0
E_{50}^{ref}	lb/ft^2	3.5 E 04	1.8 E 04	2.2 E 05	3.3 E 04
E_{oed}^{ref}	lb/ft^2	3.5 E 04	1.8 E 04	2.2 E 05	3.3 E 04
E_{ur}^{ref}	lb/ft^2	3.5 E 05	1.8 E 05	2.2 E 06	3.3 E 05
ν_{ur}		0.2	0.2	0.2	0.2
p_{ref}	lb/ft^2	2088	2088	2088	2088
m		1.0	1.0	0.5	1.0

Table 7b Hardening Soil Parameters For Calibrated Wall Model (Fill Material)

Hardening Soil Parameters	Units	Original Embankment	Granular Fill (Wall Footprint)	New Fill Material / Surcharge	Near-Face Material
γ	lb/ft^3	125	119.2	126	125
k_x	ft/day	200	200	200	200
k_y	ft/day	200	200	200	200
ϕ'	degrees	36	36	40	38
c'	lb/ft^2	10	10	10	10
ψ	degrees	0	0	0	0
E_{50}^{ref}	lb/ft^2	2.5 E 05	1.8 E 05	2.5 E 05	2.0 E 05
E_{oed}^{ref}	lb/ft^2	2.5 E 05	1.8 E 05	2.5 E 05	2.0 E 05
E_{ur}^{ref}	lb/ft^2	2.5 E 06	1.8 E 06	2.5 E 06	2.0 E 06
ν_{ur}		0.2	0.2	0.2	0.2
p_{ref}	lb/ft^2	2088	2088	2088	2088
m		0.5	0.5	0.5	0.5

3.0 Geometric Model of MSE Wall

3.1 Wall Geometry

Figure 5 shows the basic geometry of the Plaxis MSE wall model. Soils underlying the site are divided into several layers, identified as medium stiff surface clay, soft clay, stiff sandy silt, very stiff sandy clay, and semi-rigid material. The medium stiff surface clay models the dessicated Bonneville clay crust near the original ground surface, while the soft clay models the more typical soft Bonneville clay. Additional soil layers in the model replicate existing soil layers. There is also a region of granular fill beneath the toe of the wall. It should be noted that the modulus of each layer is not homogeneous, but rather it varies continuously with depth. This makes it possible to accurately model a site with relatively few soil layers.

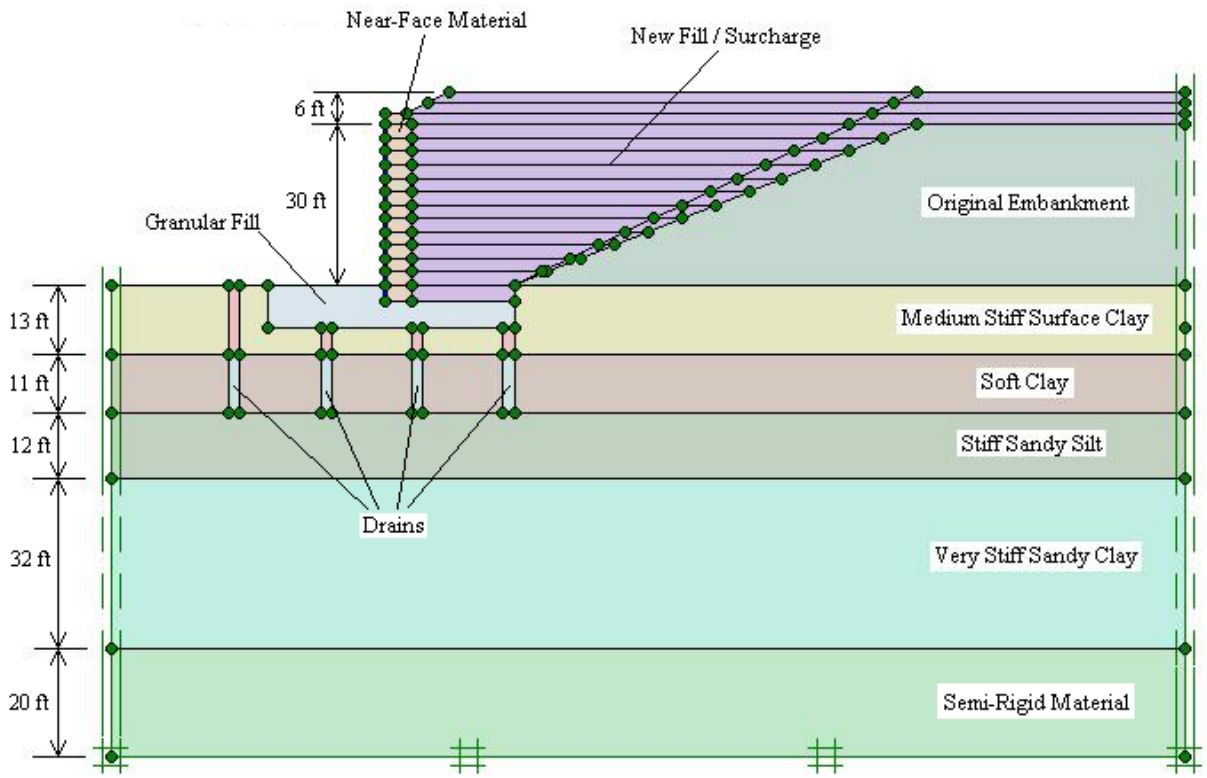

Figure 5 Simplified Geometry of Plaxis MSE Wall Model

Four drains, simulating the PVD's, extend from the ground surface or granular layer to the bottom of the soft clay layer.

The embankment consists of three parts. The original I-15 embankment, the new MSE wall fill (including surcharge), and a near-face material with slightly reduced unit weight and increased compressibility used to replicate a reduced compaction effort near the face of the wall.

3.2 Loading Sequence

A complicated loading sequence was utilized to simulate the stress history and construction sequence at the site. This sequence is explained below.

First, the site was loaded to simulate the stress history. With all embankment parts deactivated, a downward uniform load of 7000 psf was applied at the ground surface and an upward uniform load of 5000 psf was applied at a depth of 13 ft. These

uniform loads were used to simulate the combination of overconsolidation near the ground surface due to desiccation and slight overconsolidation of the entire soil profile. After consolidating under these loads, the maximum past effective vertical stress profile shown in Figure 3 was imposed at the site. Once consolidation was complete, the uniform loads were removed and the displacements reset.

Next, the original embankment plus a 6-ft surcharge at the top of the embankment, and a wedge shaped surcharge along the slope of the embankment were activated. The site consolidated under these loads.

Next the surcharge was deactivated, and site was allowed to swell. This replicates aging effects that will cause soils beneath the original embankment to be slightly over consolidated.

Next the MSE wall was constructed in 5-ft increments. Each 5-ft increment was applied instantly. After applying each increment, the wall was allowed to consolidate for a period of time equal to the time it took to construct that increment of wall. This procedure continued until the wall and surcharge were constructed.

Next, consolidation continued for an additional 120 days. Then the surcharge was removed (deactivated). At this point in time, it was anticipated that the majority of primary consolidation had taken place.

Last, consolidation continued for another 1200 days, which was approximately the time the most recent measurements were taken. This allowed a direct comparison of deformations and stresses to be made between the model and the measured wall response.

4.0 Long-term Behavior

One of the important goals of the model was to be able to represent the long-term behavior of the MSE wall. The model should be able to replicate the settlement of the wall, vertical and horizontal movement in the foundation soil, and pressure within the wall at the conclusion of primary consolidation.

4.1 Total Deformations

The total deformations of the wall model compared well to the deformations measured at the end of wall construction. Settlement of the wall was measured to be about 1.26 ft and 1.6 ft using the Sondex settlement data and the Horizontal Inclinometer data, respectively. These measurements were positioned at the base of the wall three feet from the wire mesh face. From the Plaxis model, settlement was estimated to be approximately 1.25 ft at that same point, matching the Sondex reading. Horizontal movement of the wall face was measured to be from 0.25 ft to 0.30 ft as given by vertical inclinometer data and horizontal extensometer data, respectively. The Plaxis model gives a horizontal deflection of approximately 0.22 ft at the toe of the wall. Figure 6 shows the deformed mesh at the end of primary consolidation. Figure 6a shows the deformed mesh at the true scale, and Figure 6b shows exaggerated deformations.

4.2 Vertical Deformations

Much of the calibration of the Plaxis model focused on the vertical deformation of the wall. A comparison of the Plaxis model results and the measured results for two of the Sondex tubes and one of the horizontal inclinometers is made below. Elevations above and below grade were relative to an assumed benchmark marked by a nail on the loading dock of a building near the wall site. This benchmark was assumed to have an elevation of 100 m (328.1 ft), and was far enough from the wall that no change in elevation would occur during construction. The base of the wall was determined to be elevation 325 ft, with the final wall grade at approximately 355 ft with respect to the mentioned benchmark.

4.2.1 Comparison with Sondex Measurements.

Only two of the three Sondex tubes showed measurable deformations during the construction of the wall. Sondex tube S1 was located 3 ft within the wall footprint, while Sondex tube S2 was located 8 ft from the wall face, outside the wall footprint. Both S1 and S2 showed significant vertical deformations throughout construction. The third Sondex tube (S3) was located 31 ft from the wall face, outside the wall footprint and outside the zone of PVDs. No apparent deformation occurred at this point during construction or in the three years following construction.

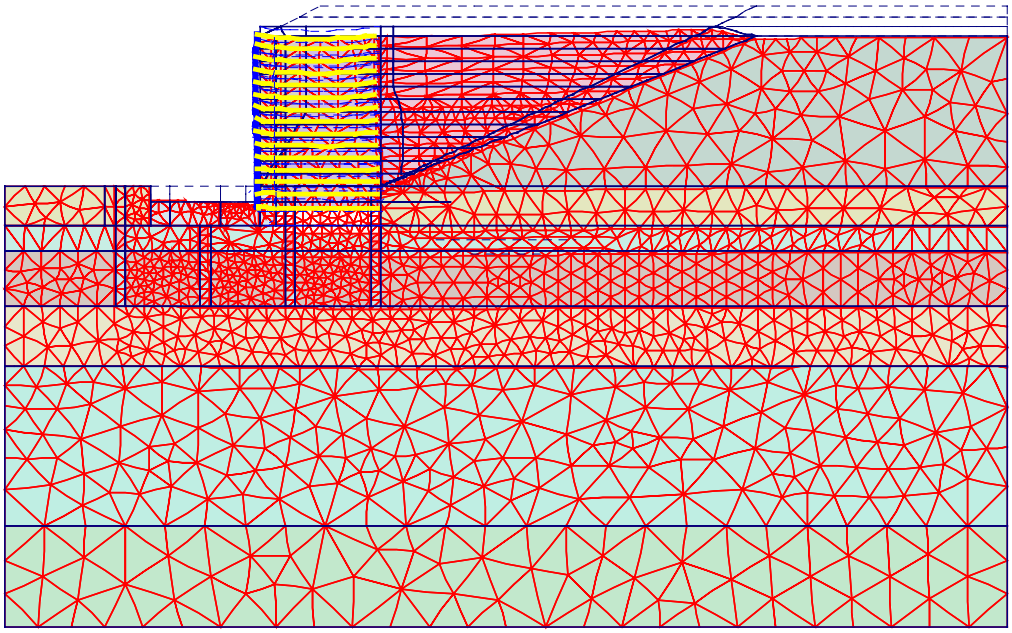

a) True Scale

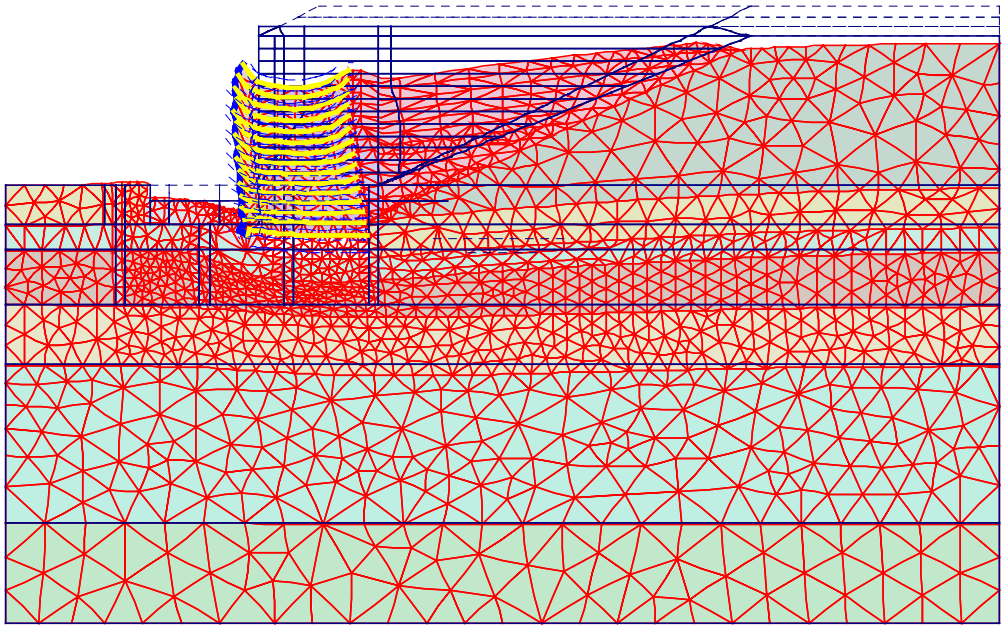

b) Exaggerated 5 times

Figure 6 Deformed Plaxis Mesh at the End of Primary Consolidation

Figure 7 shows a comparison of the Sondex tube S1 measurements taken at the end of primary consolidation compared to Plaxis model deformations at the end of consolidation. It may be noted that the maximum elevation of comparison of the model and the measured data is at the base of the wall. Measured data within the wall were given in report UT-03.11 (Instrumentation and Installation Scheme of a Mechanically Stabilized Earth Wall on I-15 With Results of Wall and Foundation Behavior). Though some strain occurred within the wall material, it was more important for the model to be valid in the foundation material, such that no comparison was made as to vertical movement in the wall backfill.

Figure 8 shows a comparison of the Sondex tube S2 measurements taken at the end of primary consolidation compared to Plaxis model deformations at the end of consolidation. The Plaxis model estimates the amount of vertical deformation of the wall with depth reasonably well for both Sondex tube locations.

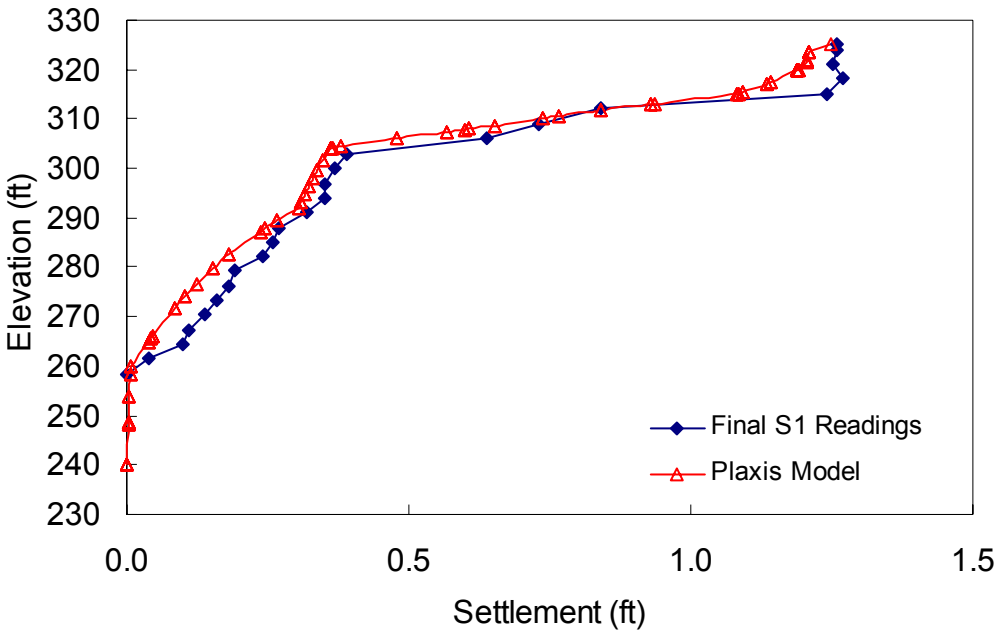

Figure 7 Comparison of Plaxis model and Sondex Tube S1 measurements of Vertical Deflection

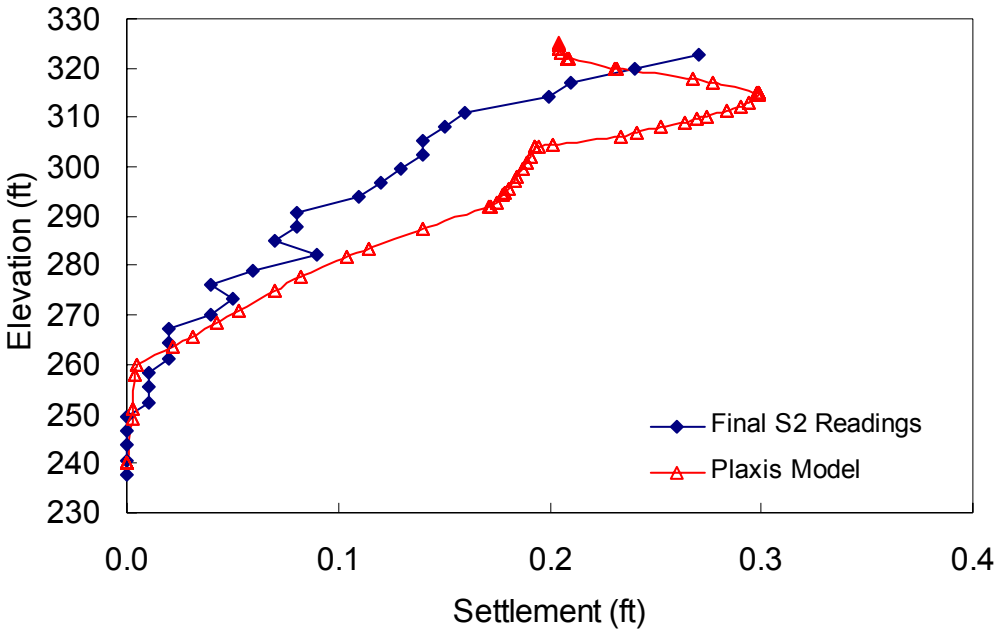

Figure 8 Comparison of Plaxis model and Sondex Tube S2 measurements of Vertical Deflection

4.2.2 Comparison with the Horizontal Inclinometer. A comparison of the vertical deformation was also made between the Plaxis model and Horizontal Inclinometer H1 that is located at the base of the wall backfill at elevation EL 325 ft. This inclinometer extends from a manhole located approximately 14 ft from the wire face of the MSE wall, and extends approximately 38 ft into the wall. The Plaxis results are compared to the measured inclinometer results in Figure 9.

The model does not currently match the measured vertical deformations very well for the horizontal inclinometer. Additional investigation and modeling will be performed in hopes of coming up with a somewhat better match of the measured data. However, the current model does do a reasonable job in predicting the vertical movement of the wall.

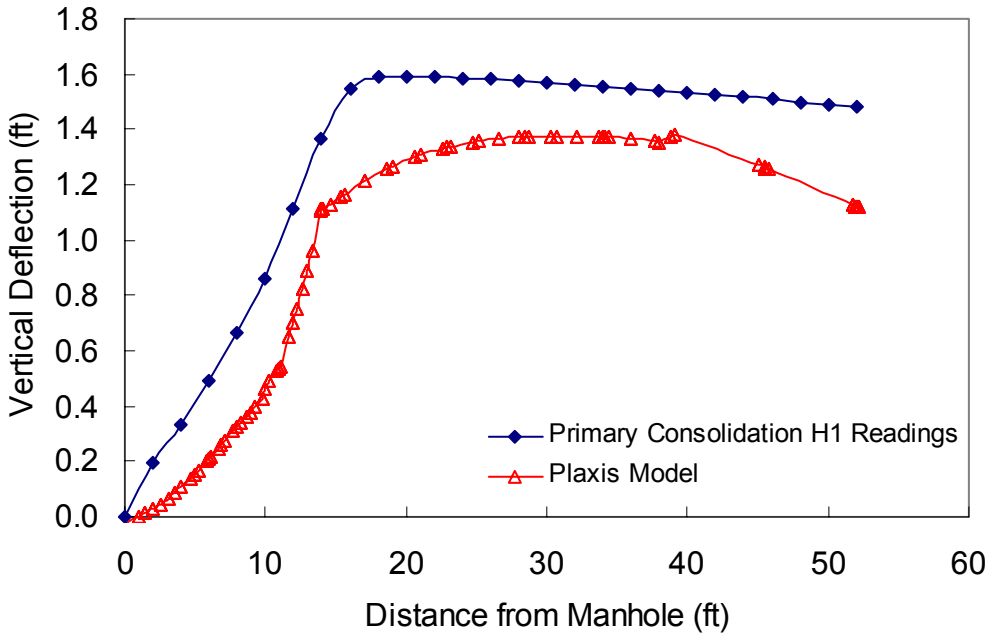

Figure 9 Comparison of Plaxis model and Horizontal Inclinometer H1 measurements of Vertical Deflection

4.3 Horizontal Deformations

Two of the three Vertical Inclinometers at the wall showed significant horizontal deformations during wall construction. Vertical Inclinometer I1 is located 3 ft from the face of the wall, within the wall footprint, and Vertical Inclinometer I2 is located 8 ft from the wall, outside the wall footprint. The third vertical inclinometer (I3), located 31 ft from the wall face, outside the wall footprint and outside the zone of PVDs, showed less than 0.06 ft of horizontal movement at the most recent measurement.

A comparison of the Plaxis model results and the measured results for inclinometer I1 and inclinometer I2 are given in Figure 10 and Figure 11, respectively. The deformations predicted by the model compare very well to those measured by the vertical inclinometer located outside the footprint of the wall (Figure 11). The reverse spike noticed between elevation 305 and elevation 292 is somehow due to the layer of silt in the model. Why the spike occurs has not yet been determined. Apart from the apparent spike, the model does a very good job at matching the measured results.

The model and the measured results do no match very well for the inclinometer located within the wall footprint. The horizontal movement in the model is very similar to the movement occurring in the measured and modeled results for the inclinometer outside the wall footprint, but does not match the measured results inside the wall footprint. The measurements taken throughout construction appear to be valid, so the difference between the model and the measured results has yet to be explained. As is quite apparent, assuming the measured results are indeed valid, the model does of poor job of replicating the horizontal deformations within the wall footprint.

Again, since the horizontal movement in the foundation was considered to be much more important than the horizontal movement within the wall, Figure 10 only compares the horizontal movement between the measured and model results for the foundation material, not comparing the movement measured within the wall to the movement modeled by Plaxis.

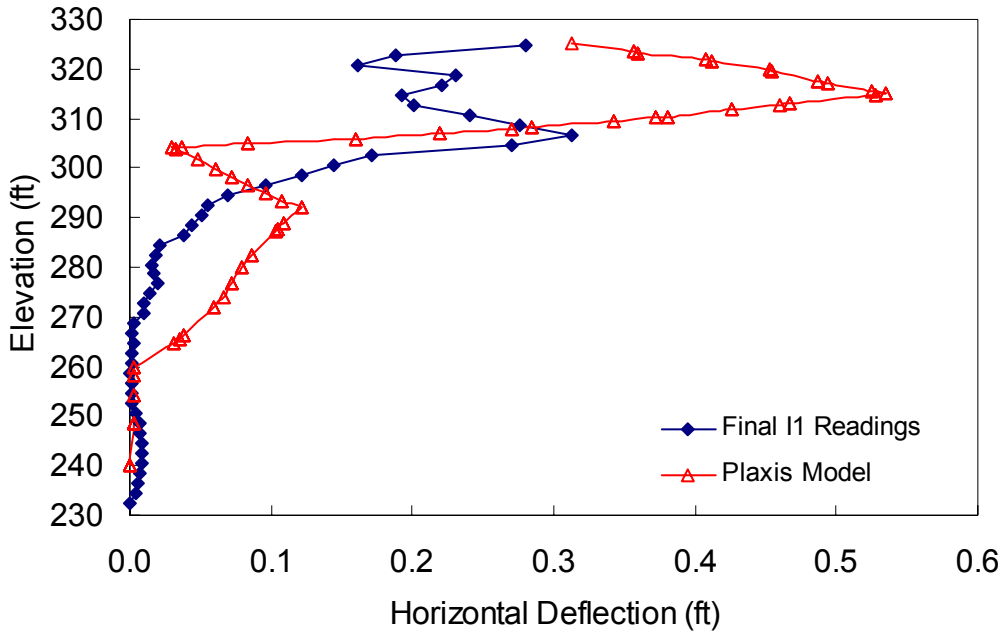

Figure 10 Comparison of Plaxis model and Vertical Inclinometer I1 measurements of Horizontal Deflection

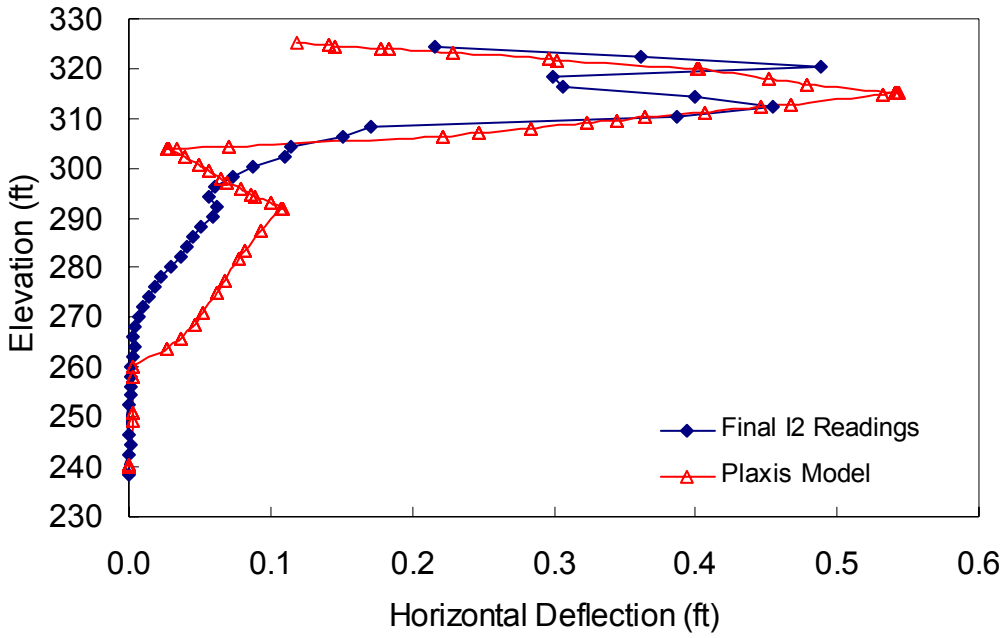

Figure 11 Comparison of Plaxis model and Vertical Inclinometer I2 measurements of Horizontal Deflection

4.4 Vertical Stresses

Pressure Plates were placed in the wall approximately 6 ft vertically from the base of the wall, located from 1 ft inside the wall footprint to 30 ft inside the wall footprint. The measured values (with surcharge applied) at the end of primary consolidation are compared to the Plaxis model values in Figure 12.

The Plaxis model does a fair job of replicating the vertical stresses within the wall. The decreased stress occurring near the wall face is reproduced quite well, though the model still overpredicts the stress near the face. The position of the peak stress occurring 6 to 8 ft from the wall face is modeled very well, but the magnitude of this peak stress is underpredicted significantly. The stresses further into the wall are approximated quite well by the Plaxis model.

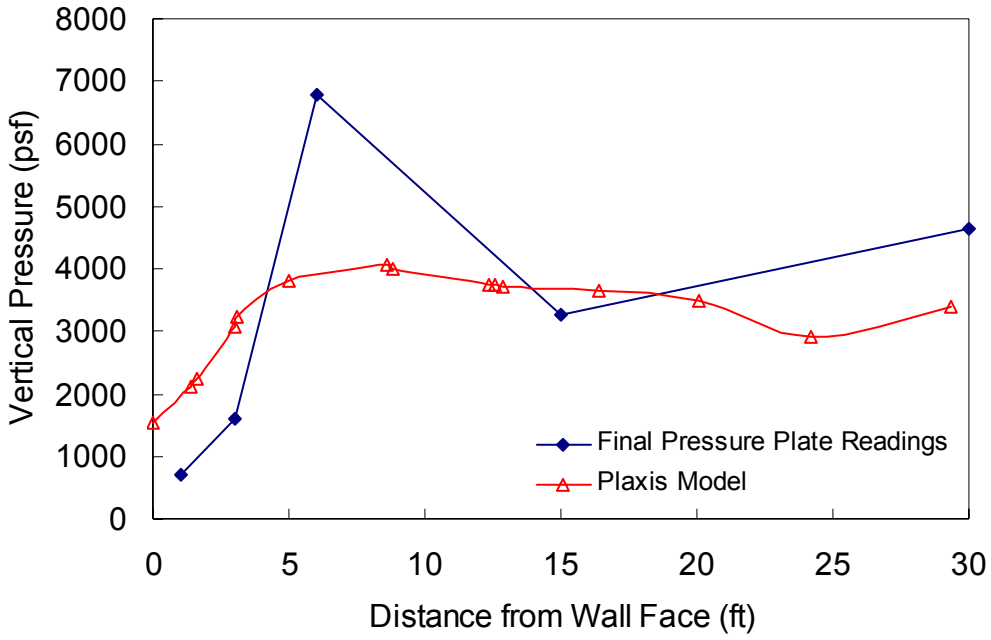

Figure 12 Comparison of Plaxis model and Pressure Plate measurements of Vertical Pressure

5.0 Time Settlement Behavior

5.1 Time Settlement Curves

The Plaxis model time settlement behavior was calibrated to the actual wall by matching the time settlement curves at Sondex 1 (S1). A comparison between the measured and calculated settlement curves is shown in Figure 13. Figure 13a shows the time settlement up to 200 days and Figure 13b shows the long-term time settlement. Construction records were used to determine the staging sequence of the analytical model. The match between the model and measurements is extremely close up until 200 days. This time corresponds with the end of primary consolidation. After this time there is no additional settlement in the analytical model while the measurements continue to show some settlement. This is expected because the analytical model does not include secondary consolidation or creep.

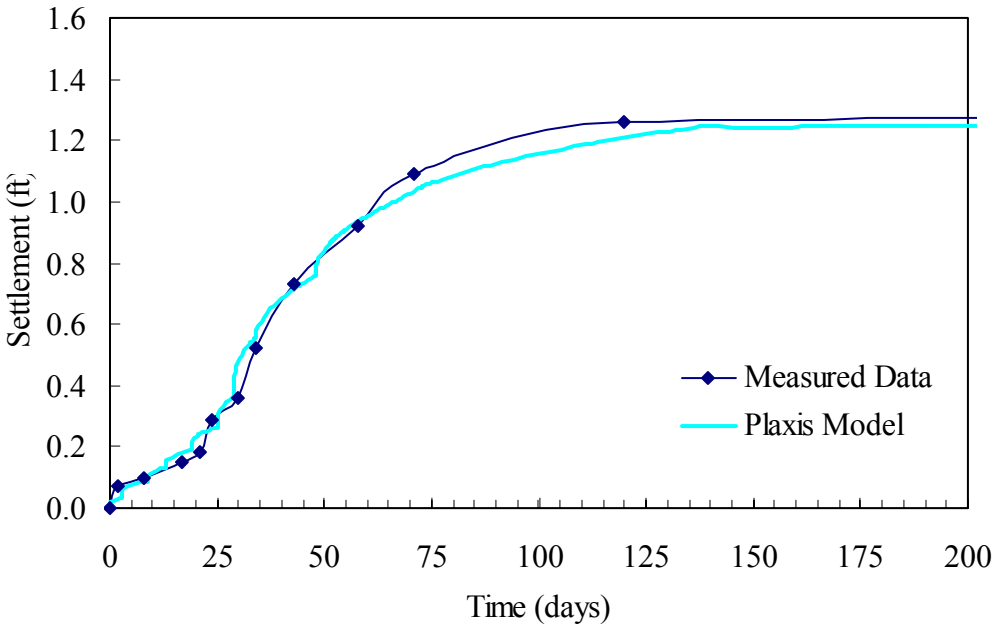

a) First 200 days after beginning of construction

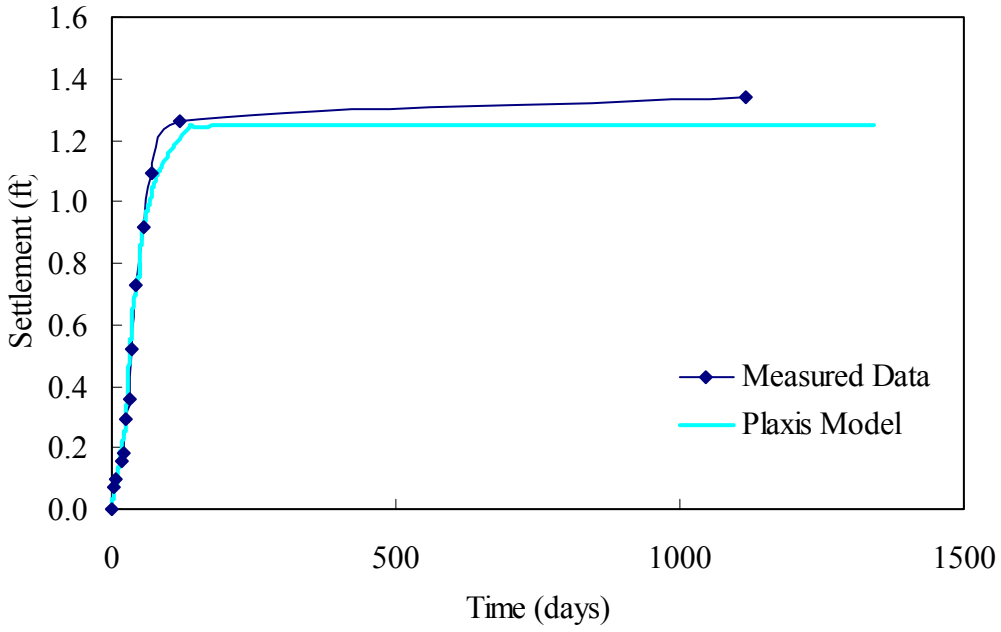

b) First three years after beginning of construction

Figure 13 Time Settlement plot comparing Plaxis model with measured results of settlement at the Base of the MSE Wall

The close agreement between analytical and measured time settlement curves gives a high degree of confidence in the models' pore pressure dissipation and settlement evaluations.

5.2 Pore Pressure Dissipation

A series of figures showing the excess pore pressures in the foundation are plotted in Figures 14 – 21. These plots show the excess pore pressures during construction and continue through the end of primary consolidation. The highest excess pore pressure that occurred during staged construction was 1850 psf. The contour interval for each figure is the same for easy comparison.

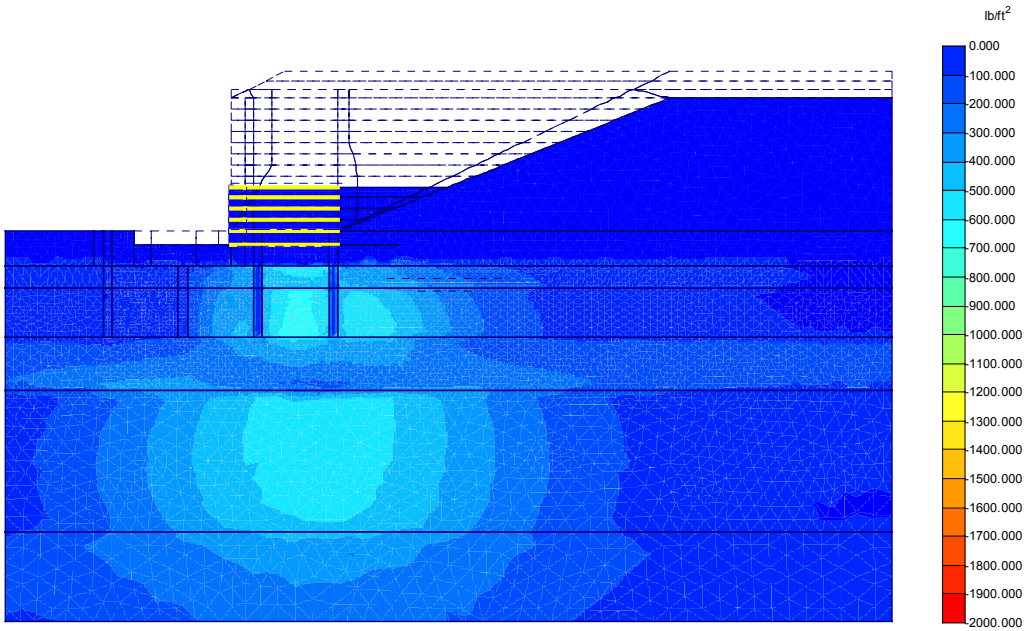

Figure 14 Excess Pore Pressures at Lift of 10 ft

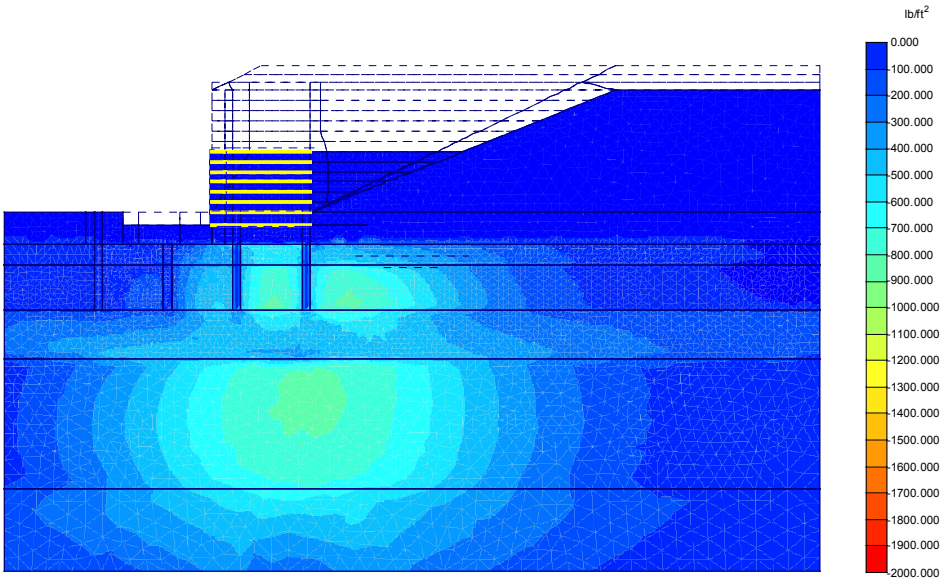

Figure 15 Excess Pore Pressures at Lift of 15 ft

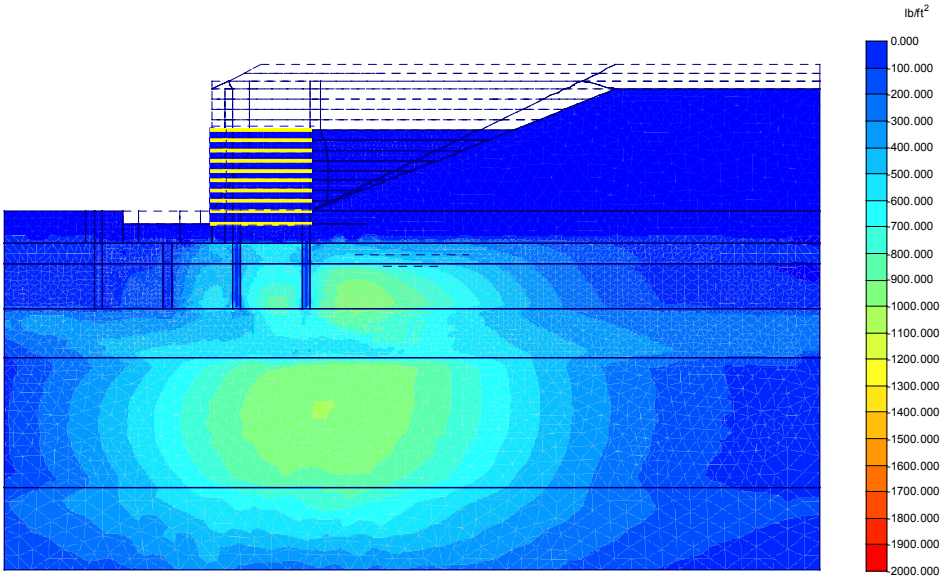

Figure 16 Excess Pore Pressures at Lift of 20 ft

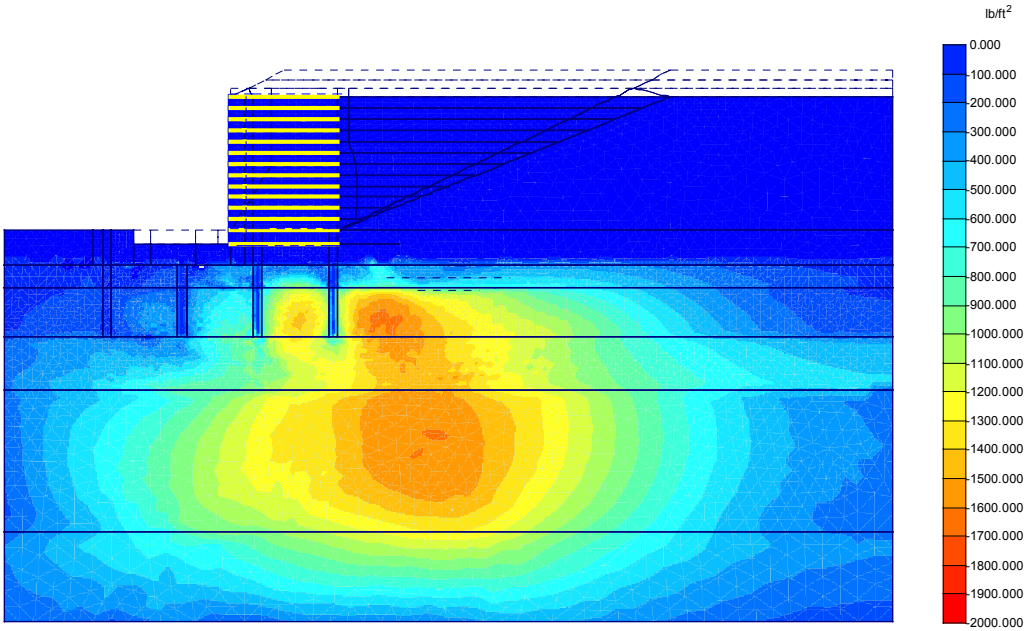

Figure 17 Excess Pore Pressures at Lift of 30 ft

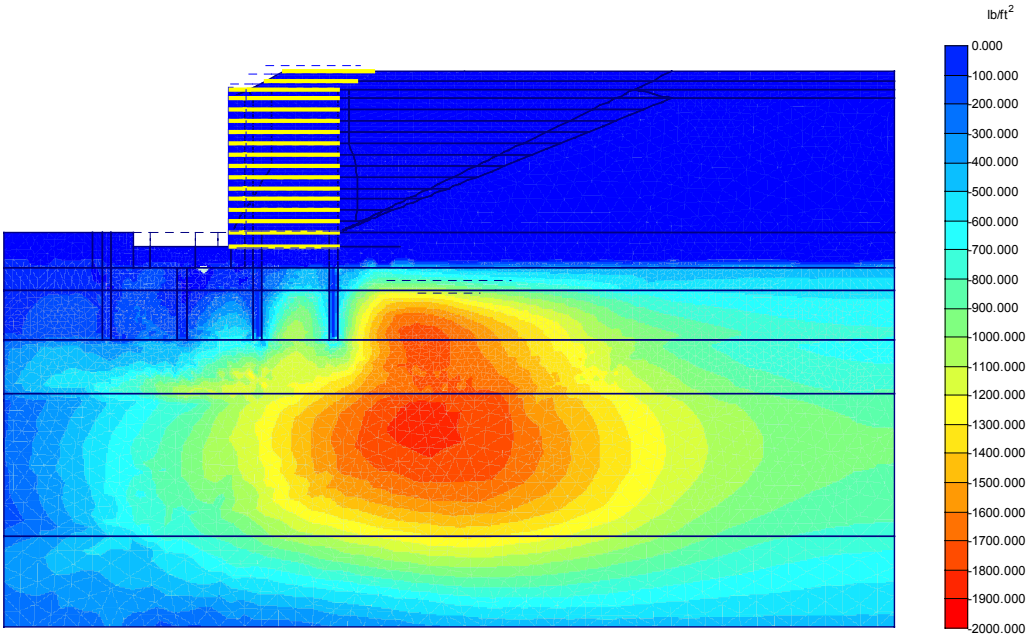

Figure 18 Excess Pore Pressures at Lift of 36 ft

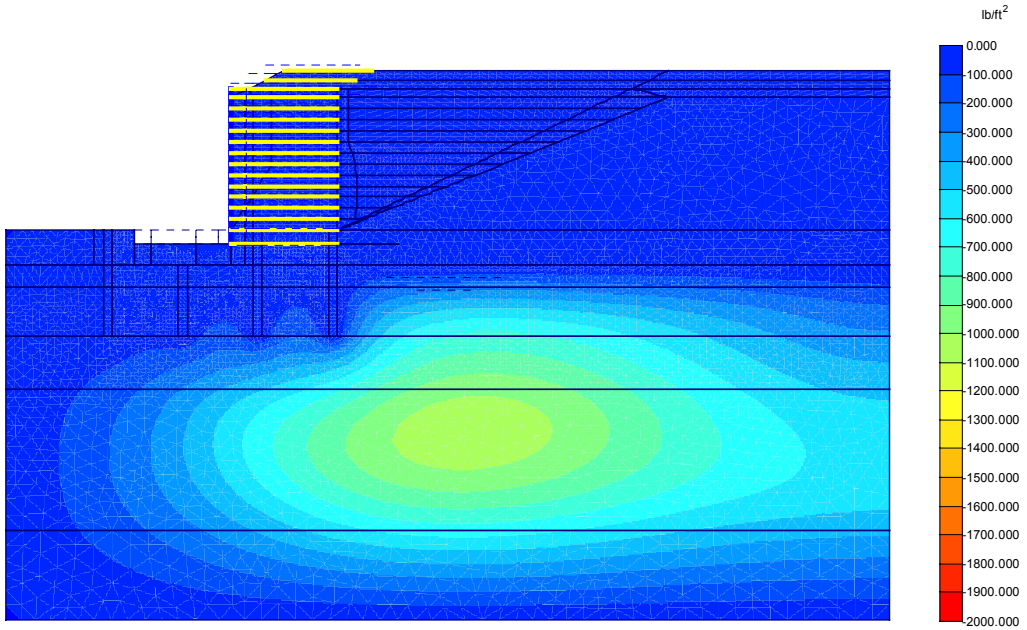

Figure 19 Excess Pore Pressures 45 days after Placement of Surcharge

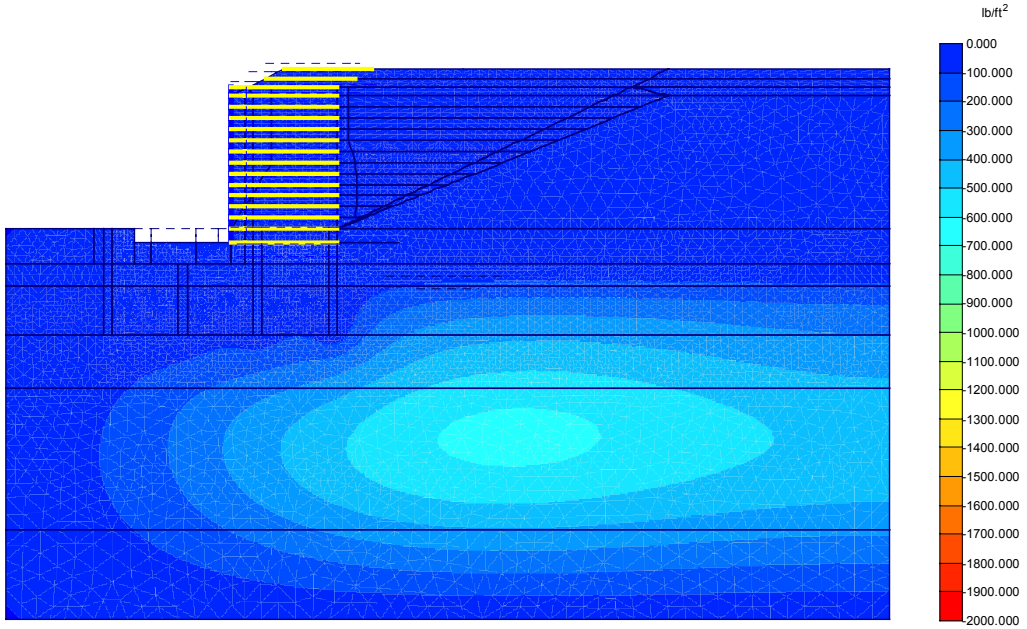

Figure 20 Excess Pore Pressures 90 days after Placement of Surcharge

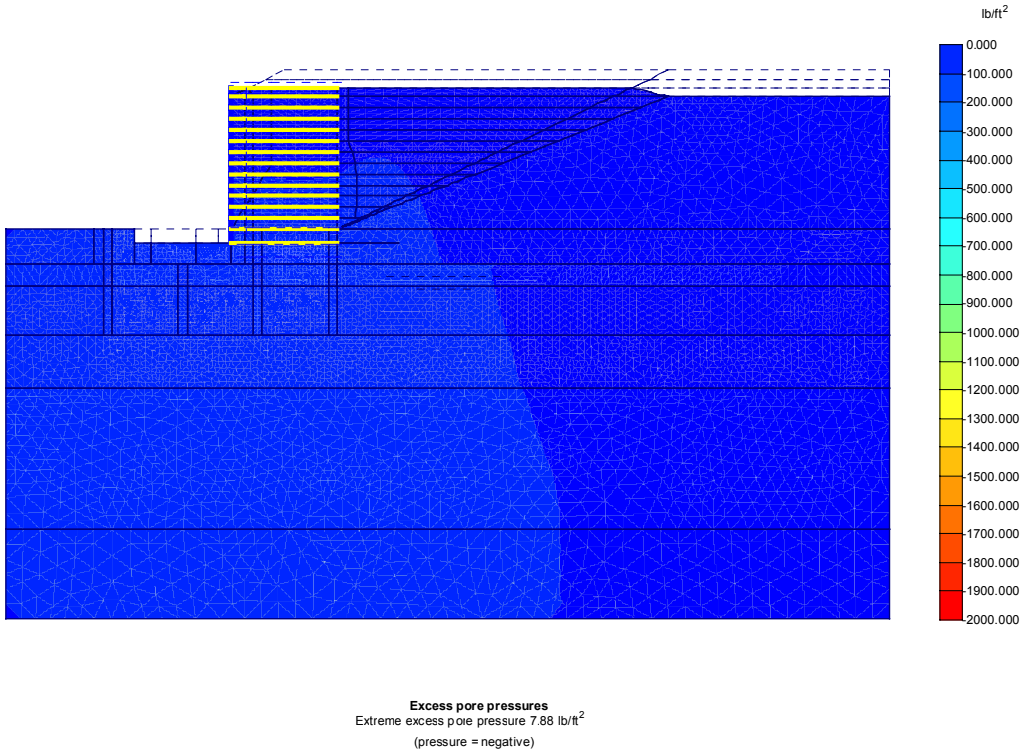

Figure 21 Excess Pore Pressures 100 days after Removal of Surcharge

Often undrained strength parameters are used to evaluate the stability of embankments. This assumes that no drainage is allowed. This condition can also be evaluated in Plaxis by applying the entire embankment instantly. The excess pore pressures from this loading condition are shown in Figure 22. Note that **the contour interval was adjusted** from the plots showing the staged construction, since the pore pressure magnitude was much higher. The highest pore pressure that occurred during instantaneous construction was 7030 psf, or more than four times the maximum excess pore pressure that occurred during staged construction. However, this maximum value occurred at a very small area at the base of one of the equivalent drains. A more appropriate maximum pore pressure for the foundation material occurs deeper in the foundation at a location similar to where the maximum value occurs for staged construction. This value of approximately 3000 psf is more indicative of the maximum pore pressure that would develop if instantaneous construction was possible.

Comparing this value (3000 psf) to the 1850 psf that developed during staged construction indicates that an undrained analysis would lead to pore pressures that were 60 percent higher than the maximum pore pressures that develop during the staged construction process. This indicates that the use of undrained strength parameters without accounting for pore pressure dissipation is extremely conservative for loading conditions like those encountered at this site.

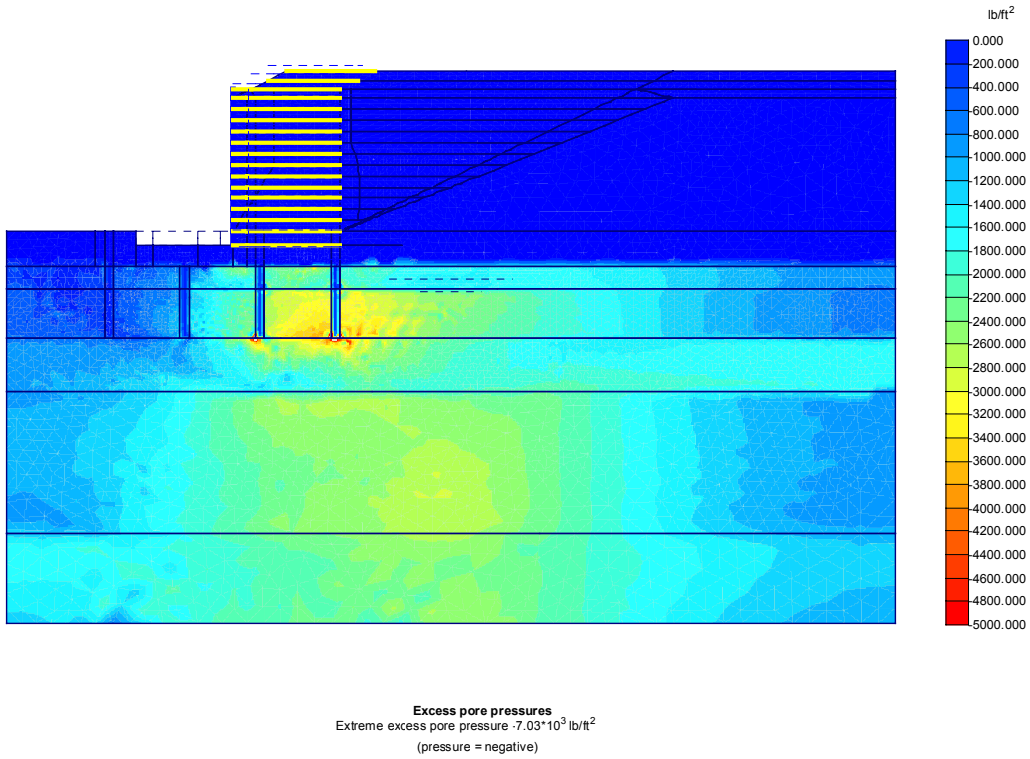

Figure 22 Excess Pore Pressures after Instantaneous Wall Construction

Figure 23 shows plots of maximum excess pore pressure versus time for staged and instantaneous construction. For instantaneous construction the highest excess pore pressure occurs at time = 0. For the staged construction the excess pore pressures reach a peak at 47 days, corresponding to the time at which the surcharge load was applied to the wall.

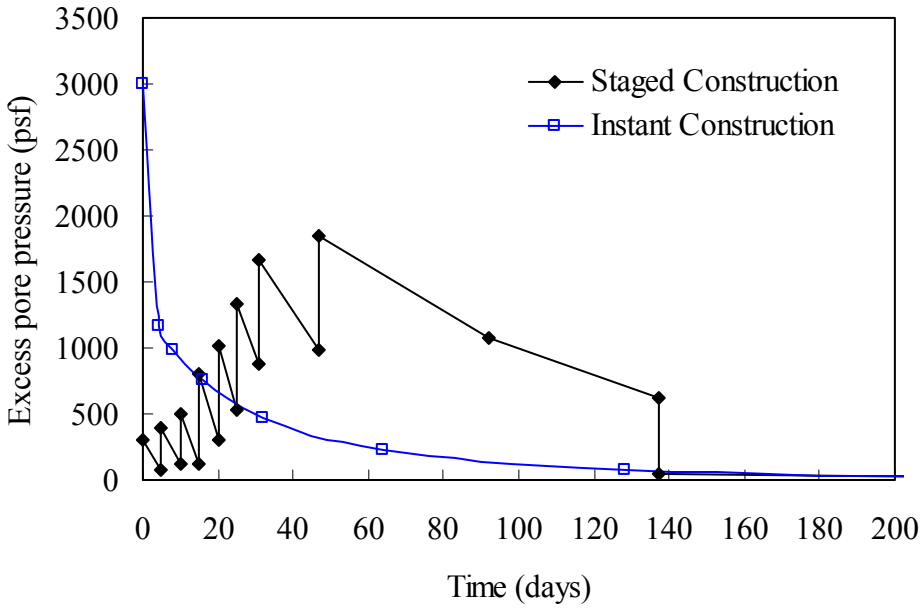

Figure 23 Excess Pore Pressures versus Time for Instantaneous and Staged Construction

It should be noted that the stepwise function for the staged construction is entirely a function of the loading sequence for the model. Lifts were chosen that corresponded well with the position of the reinforcement within the soil (ie. five foot lifts allowed for exactly two reinforcement layers to be added, complete with backfill.) These lifts were applied instantaneously, as mentioned earlier, then consolidation was allowed for the time during which construction of that lift actually occurred. Thus, the model does not exactly follow the sequence of construction, but is a close approximation of the construction process.

6.0 Soil-Reinforcement Interaction

6.1 Introduction

The interaction between the backfill material and the bar mat reinforcement in the MSE wall is a complex three-dimensional phenomenon. Friction along the longitudinal

bars, combined with passive resistance from the transverse bars, provide the soil-reinforcement interaction for the system. Plaxis does not have the capacity to fully model such complicated three-dimensional phenomena, therefore, a highly simplified model was employed. This simplified model is adequate for modeling the external stability of the wall, where the soil reinforcement plays a minor role. However, the model is inadequate for detailed analysis of the internal stability of the wall.

Modeling this interaction was rather difficult, for several reasons. First, the amount of reinforcement within the wall was not constant throughout the wall height. Although the center-to-center spacing of the bar mats was constant (5.5 ft), the width of the bar mats varied depending on the position of the reinforcement within the wall. The mats varied from being 1.5 ft wide (four longitudinal bars spaced at 0.5 ft) to 2.5 ft wide (six longitudinal bars spaced at 0.5 ft). This also implies that the width of soil between successive bar mats (ie. "unreinforced soil") varies from 3.0 ft to 4.0 ft, depending on the width of the bar mats at a particular position.

Another difficulty was the fact that the reinforcement model (geotextile model) in Plaxis only allows the property EA (Young's modulus times the cross sectional area) for the sheet reinforcement. It was determined that the best approach was to use an equivalent EA term for a given layer of reinforcement, using an appropriate modulus of elasticity for steel and the appropriate cross sectional area for the longitudinal bars for a given layer of reinforcement.

The final input value that influenced the behavior of the soil-reinforcement interaction was the R_{inter} value. This value is the strength reduction factor for the interfaces, and is a property of the soil that is in contact with the reinforcement. This value allows the strength of the interface to be a function of the soil strength (Plaxis, 1998).

The Plaxis user's manual (1998) notes that R_{inter} may be assumed to be on the order of 0.67 for sand-steel contact, in the absence of more detailed information. Numerous iterations were made to determine the effects of the R_{inter} values on the behavior of the reinforcement as the wall was constructed. It was determined that the

strength reduction factor does play a significant role, especially when examining the position and magnitude of the maximum tension within the reinforcement.

6.2 Reinforcement Parameters

In comparing the measured tension during construction to the tension in the reinforcement in the model, it was found that the predicted tension distribution and the maximum tension observed in a given mat did not compare very well to the measured values. The maximum tension significantly overestimated the measured values in the lower portion of the wall, while underestimating the tension in the upper section of the wall, as shown in Figure 24. Table 8 summarizes the values used to model the soil-reinforcement interaction.

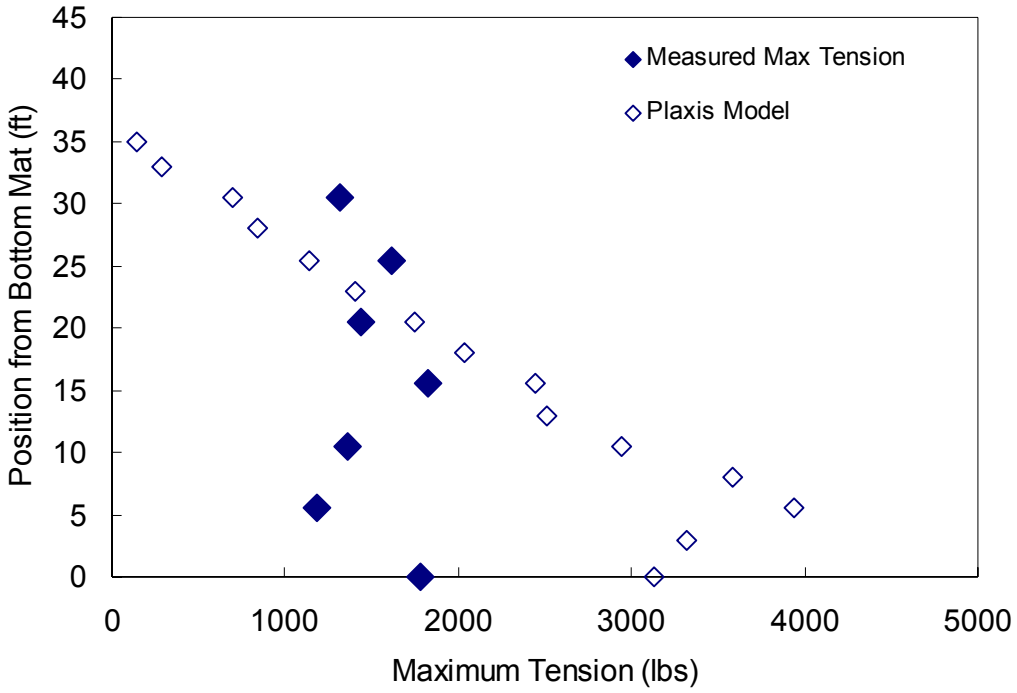

Figure 24 Plaxis Model Maximum Tension versus Measured Maximum Tension Plotted with Respect to Reinforcement Position within Wall

Table 8 Reinforcement Parameters

Description of Bar Mat	EA Value for Geotextile Reinforcement (lb/ft)
Four-Bar Longitudinal Bar Mat Near Wall Face	2.07 E 05
General Four-Bar Longitudinal Bar Mat	2.07 E 06
Five-Bar Longitudinal Bar Mat Near Wall Face	2.59 E 05
General Five-Bar Longitudinal Bar Mat	2.59 E 06
Six-Bar Longitudinal Bar Mat Near Wall Face	3.105 E 05
General Six-Bar Longitudinal Bar Mat	3.105 E 06

A three-foot length of reinforcement near the face of the wall was given a lower EA value (by a factor of 10) than the remaining reinforcement to make it more compliant. Initial model runs produced higher-than-reasonable tensions near the wall face. Making the reinforcement more compliant near the face allowed more reasonable values.

Figure 25 shows a comparison of the measured tension and the Plaxis model tension in bar mat PL5 (as given in the Instrumentation report, UT-03.11, 2003), which is located approximately 20 ft above the base of the wall. As seen, Plaxis overpredicts the maximum tension occurring in this bar mat, and significantly overpredicts the tension for the reinforcement from the wall face to 10 ft from the wall face.

Thus, the Plaxis model does not model the bar mat reinforcement very well. No combination of reinforcement and soil properties was found that replicated the measured tension in the bar mats for the entire wall height. Since the effects of the reinforcement were considered to be minimal with respect to foundation deformation and overall wall response, a more effective model of the reinforcement was not considered necessary for an external stability analysis of the wall. However, it was determined that an internal stability analysis of the wall and reinforcement would not be useful without an improved reinforcement model.

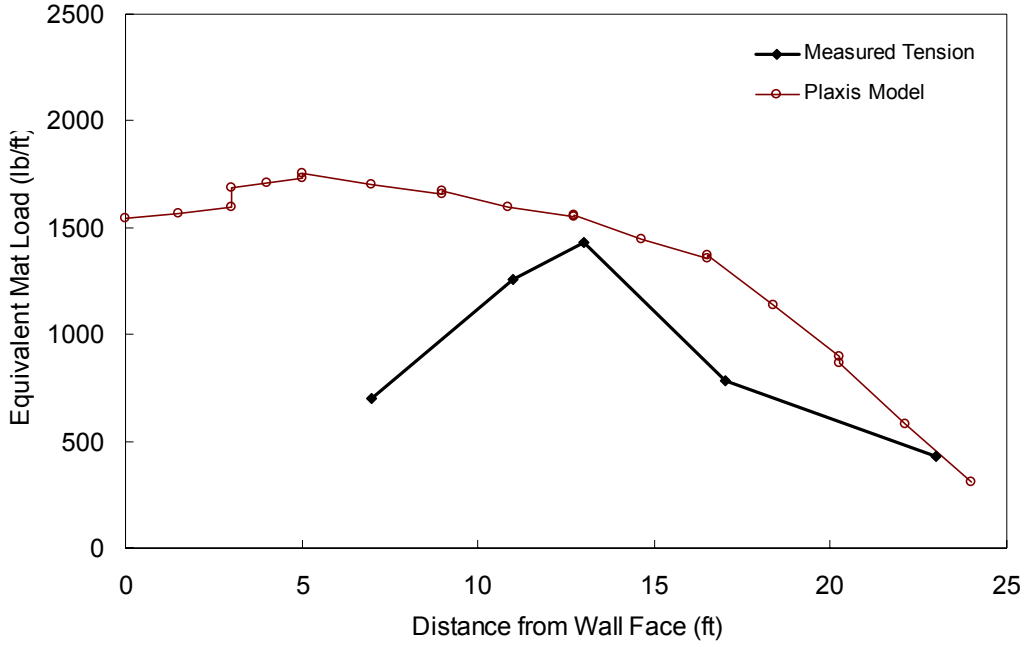

Figure 25 Plaxis Model Tension versus Measured Tension in Bar Mat PL5

7.0 Stability versus Time

7.1 Global Stability Analysis

Once a model was constructed that adequately replicated the measured behavior of the wall and foundation material, a stability analysis was performed to evaluate the stability of the wall. The stability was investigated using the phi-c reduction method in the Plaxis software. Using this procedure, a factor of safety is calculated by monitoring deformations at points within the model while reducing the soil's strength parameters (tan (phi) and c) by a factor of ΣMsf. This factor is defined as "the quotient of the original strength parameters and the reduced strength parameters" at the point at which failure is considered to occur (Plaxis, 1998). When the wall stability becomes critical, deformations will become large, and the value of ΣMsf represents the factor of safety.

Figure 26 compares the global stability (as factor of safety ΣMsf) versus time for the construction sequence of the wall. The construction sequence given was estimated

from field notes during the project. Also shown in Figure 26 is the factor of safety versus time as calculated for the theoretical instantaneous construction mentioned previously. As expected, the instantaneous construction had a much lower initial factor of safety due to much higher excess pore pressures in the foundation material. However, as consolidation occurs, the instantaneous factor of safety converges to a value nearly identical to the long-term factor of safety for the staged construction.

It should be noted that the factor of safety calculated by Plaxis for the original I-15 embankment was 2.03, with a failure surface that will be shown later. The reason for the increase in the factor of safety during the construction of the wall is that initially the wall behaves as a berm for the embankment, forcing the failure surface further up the embankment, and increasing the factor of safety. However, when the wall becomes high enough, the failure surface is forced into the foundation soil, which again decreases the factor of safety. The long-term factor of safety for the wall is 1.69 for the staged construction at the final embankment height.

Figure 27 compares the external stability (as a factor of safety) as a function of the wall height for the construction sequence of the wall. The significance of the initial 15 ft of wall acting as a berm for the original embankment is evident in this figure. Slight increases in the factor of safety as the soil consolidates at a given wall height are due to increases in the soil strength with consolidation. The plot follows the construction sequence, where the wall was built to a height of 36 ft (which included approximately 6 ft of surcharge material), after which the surcharge was removed to the final grade of 30 ft. This explains the two lines between 30 ft and 36 ft.

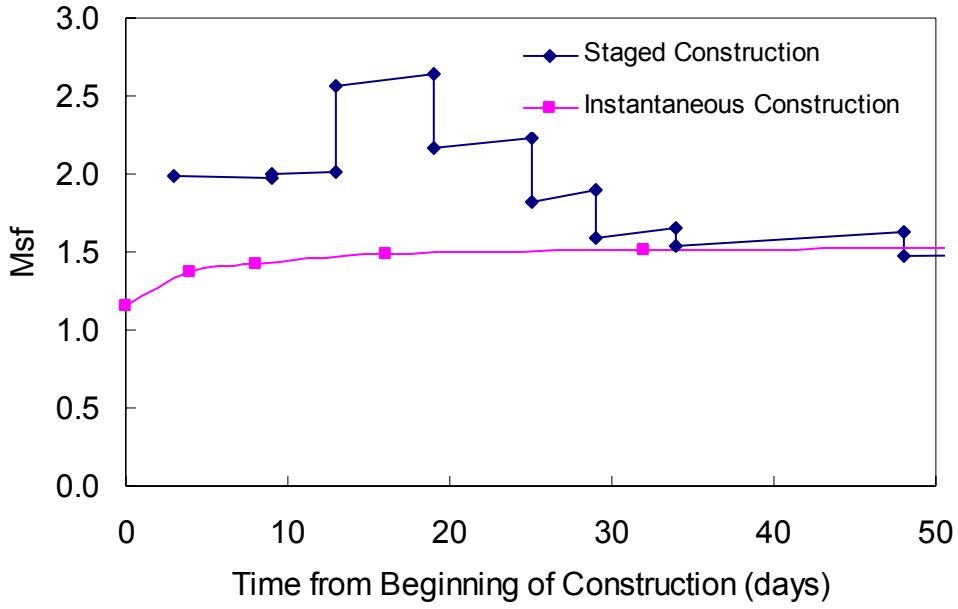

a) First 50 days

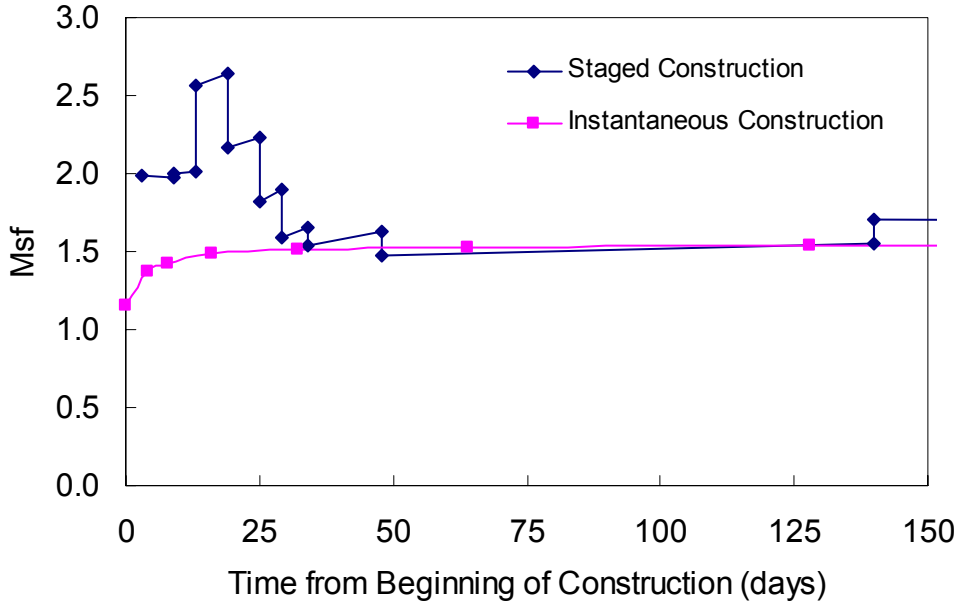

b) First 150 days

Figure 26 External Stability of MSE Wall versus Time

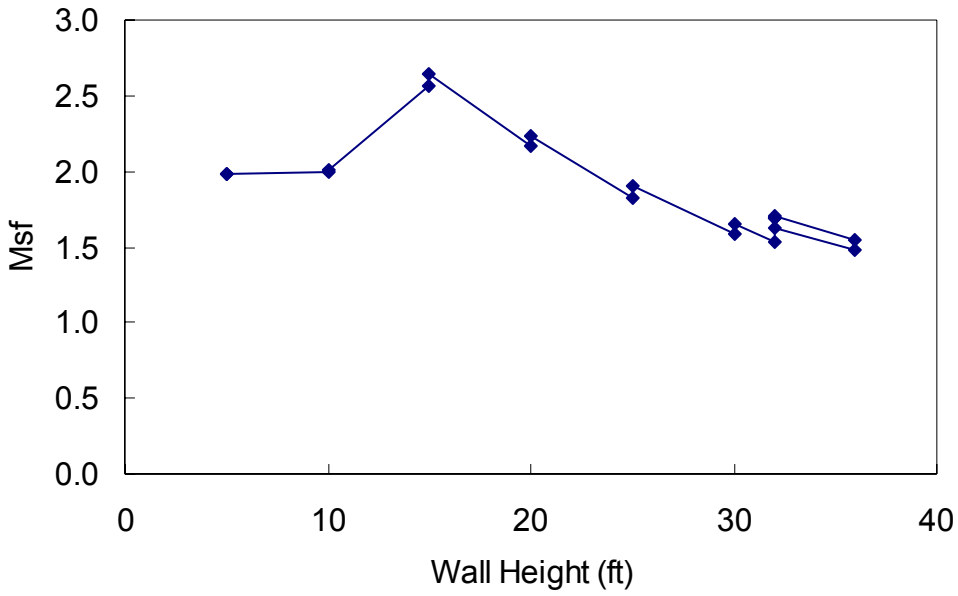

Figure 27 External Stability of MSE Wall as a Function of Wall Height

Figures 28 through 35 show the progression of the failure surfaces through the staged construction process. These figures show the deformation vectors calculated during the phi-c reduction procedure. These vectors show the extent of the sliding soil mass and the location of the failure surface. As noted, initially the failure surface was a surficial failure in the original embankment. The factor of safety for the original embankment was 2.03. The initial several lifts of the wall provided a berm for the embankment failure, which increased the factor of safety from about 2.0 to a maximum of about 2.6 when the wall height was 15 ft. However, as construction progressed, and as the effect of the berm was overcome, the failure surface was forced into the foundation soil, as seen in the later figures. The factor of safety dropped to a minimum value of 1.475 when the surcharge was applied, then increased to a final value of 1.686 for the final wall configuration as consolidation occurred.

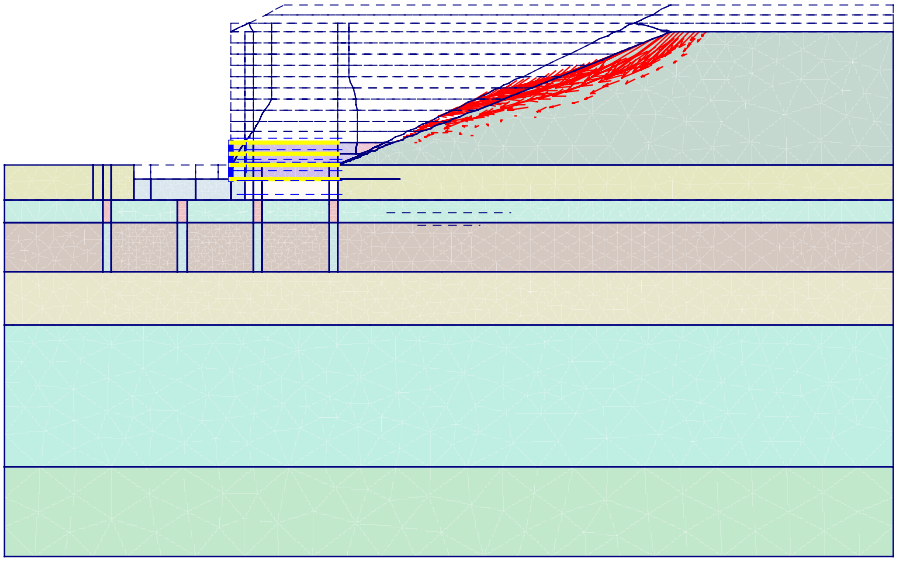

Figure 28 Failure Surface after Phi-C Reduction for 5 ft Wall

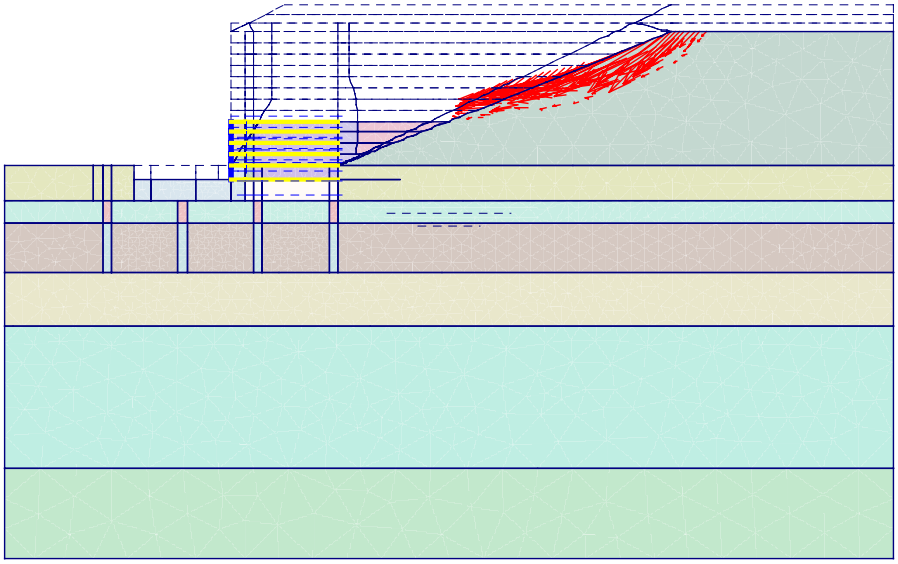

Figure 29 Failure Surface after Phi-C Reduction for 10 ft Wall

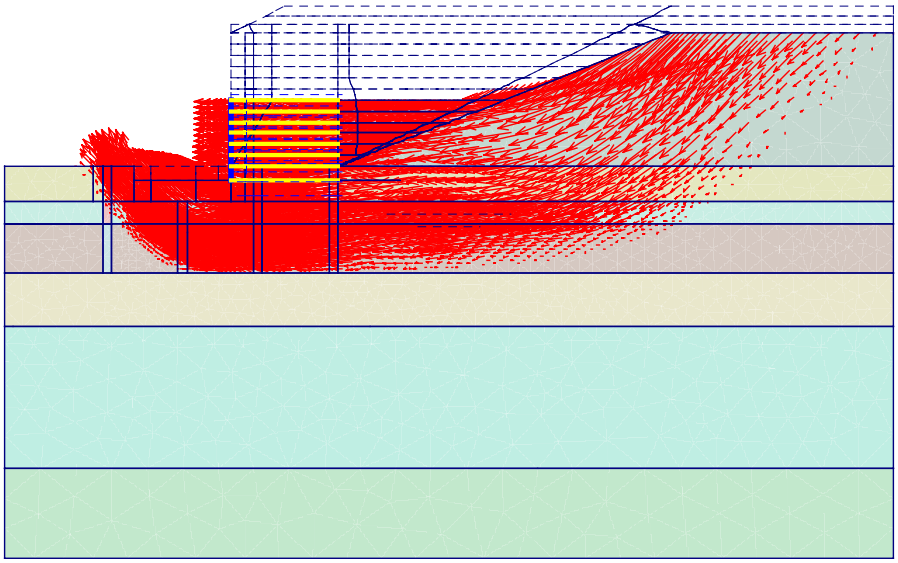

Figure 30 Failure Surface after Phi-C Reduction for 15 ft Wall

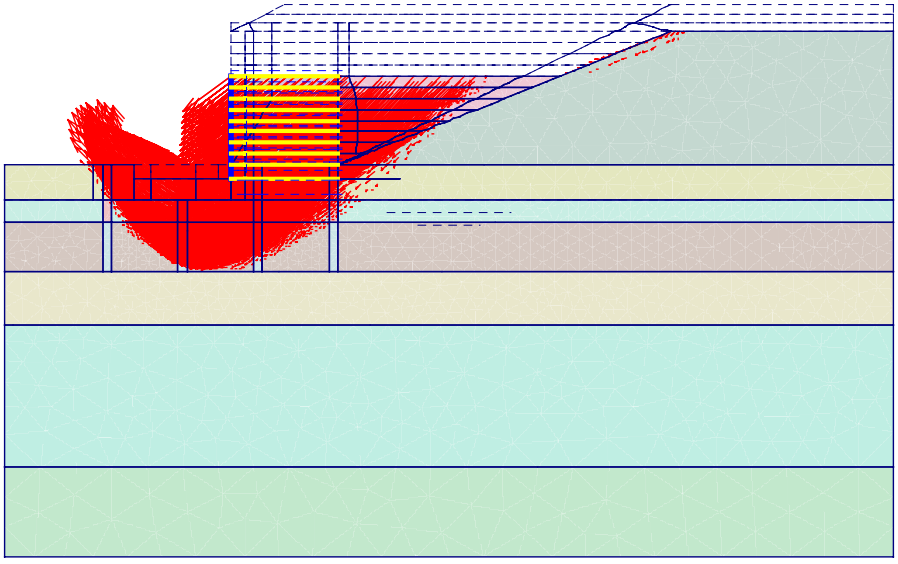

Figure 31 Failure Surface after Phi-C Reduction for 20 ft Wall

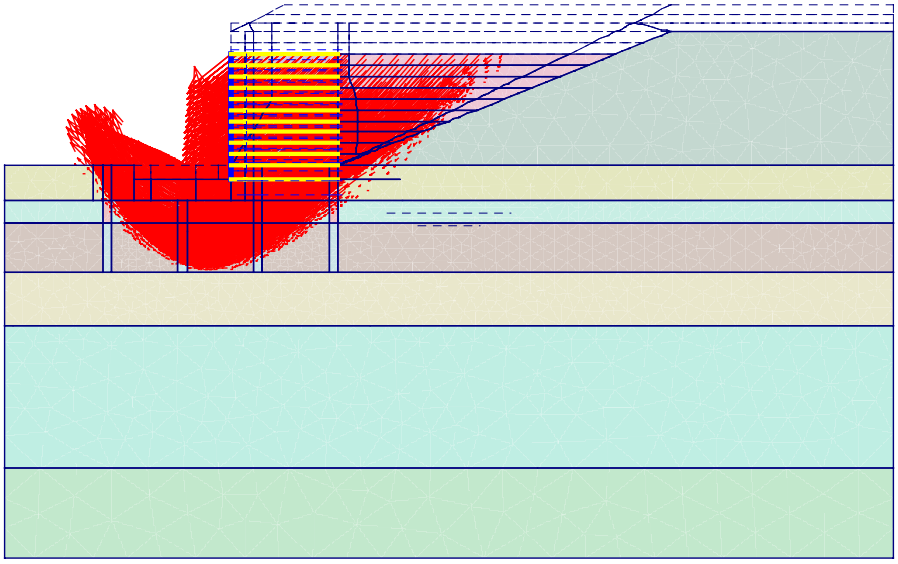

Figure 32 Failure Surface after Phi-C Reduction for 25 ft Wall

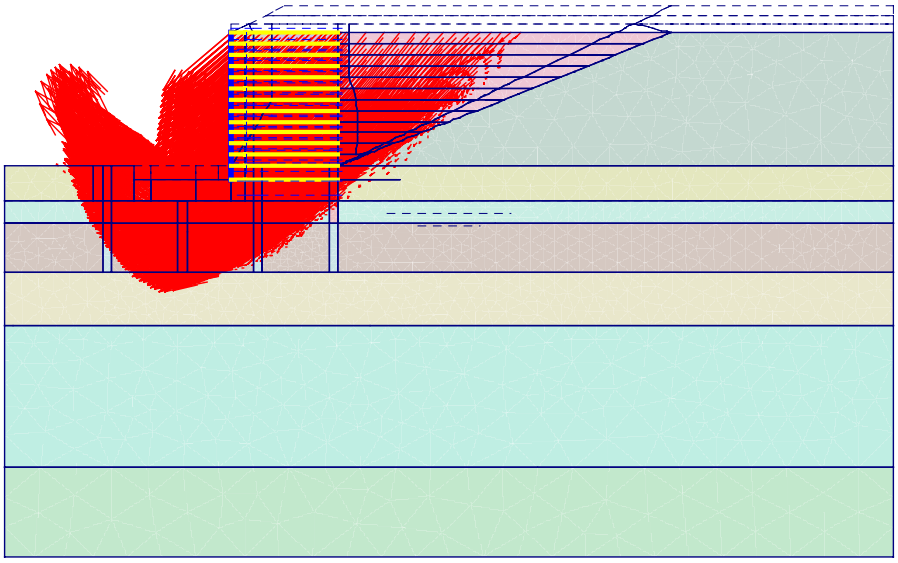

Figure 33 Failure Surface after Phi-C Reduction for 30 ft Wall

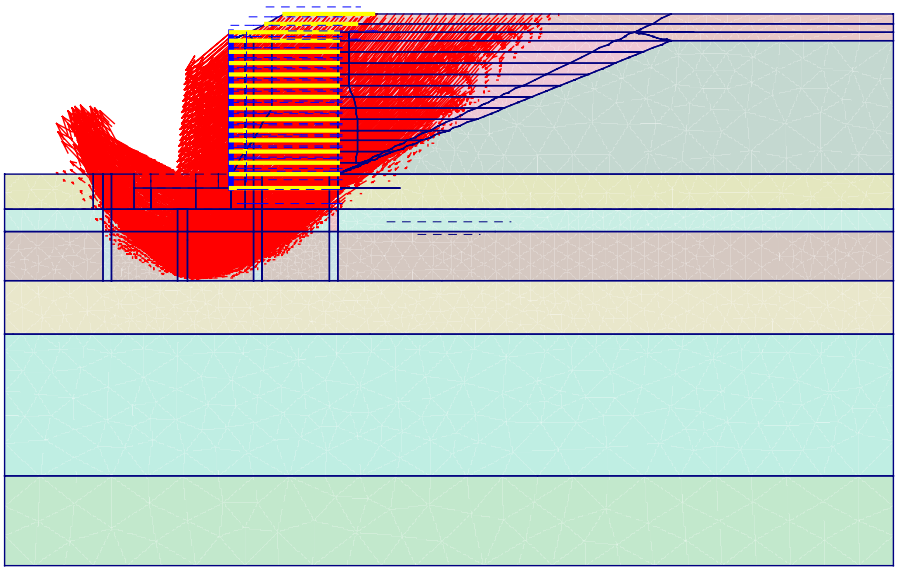

Figure 34 Failure Surface after Phi-C Reduction for Wall with Surcharge

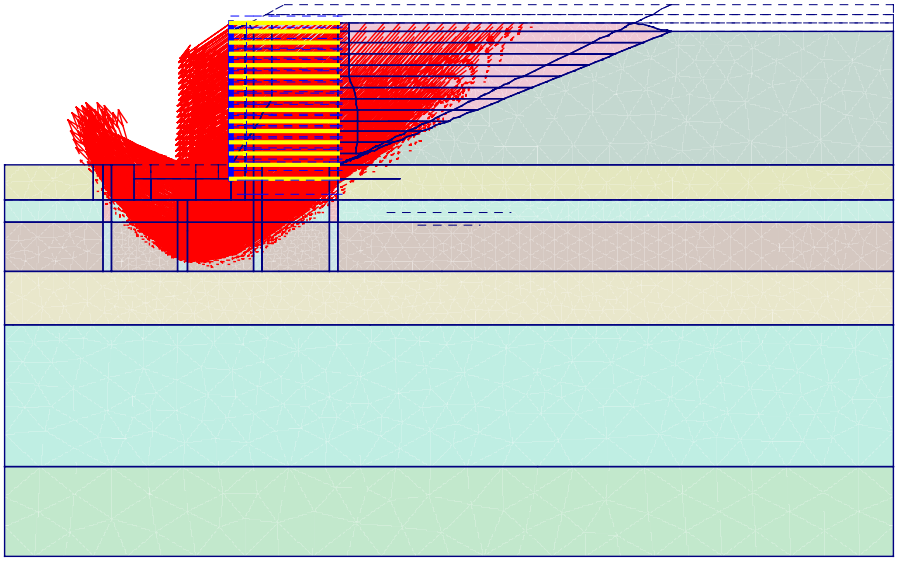

Figure 35 Long-term Failure Surface after Phi-C Reduction for Final Wall

Of particular note is the shape of the failure surface for the final wall configuration. As seen in Figure 35, for example, the failure surface has a V-shape, with total movement being downward and away from the original embankment in the backfill material and the foundation material beneath the wall backfill, and with total movement being upward and away from the wall in the foundation material outside the wall footprint. It is noteworthy that such a failure surface might not be predicted using some automated traditional slope stability analyses, where a circular or spiral failure surface is typically used to compute a factor of safety. Slope stability software packages that allow for manually specified failure surface could better approximate such a failure mechanism, assuming such a surface was anticipated by the user. For this case, it appears that a traditional slope stability approach might not be conservative, especially if the stability analysis required a circular or spiral failure surface.

Figure 36 shows the failure surface for the instantaneous construction of the wall. It should be noted that the minimum factor of safety for the instantaneous construction (immediately after applying the load) is a value of 1.16, which is significantly less than the factors of safety calculated during the staged construction process.

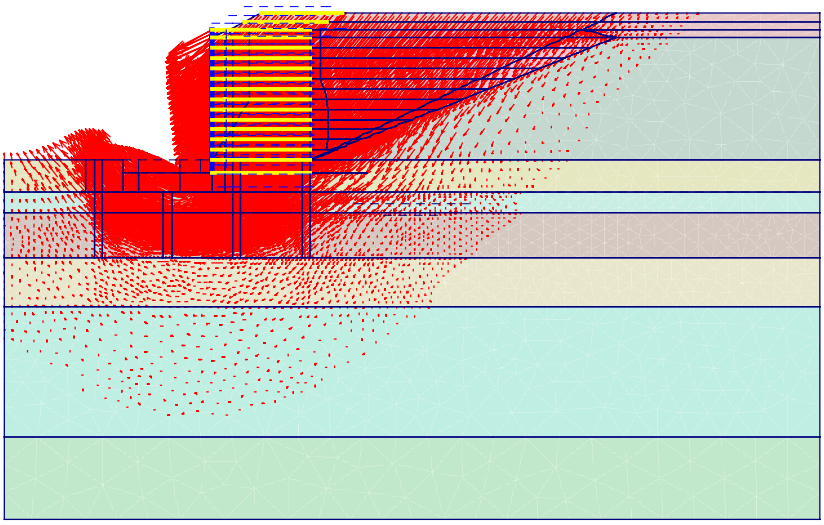

Figure 36 Failure Surface after Phi-C Reduction for Instantaneous Wall Construction

7.2 Additional External Stability Analyses

Once the analysis of the global stability of the wall was completed, an analysis of some additional failure modes was performed. As discussed in section 6.1, the Plaxis model is unable to adequately model the complex, three-dimensional behavior of steel bar mats. With this limited and simplified model of the soil-reinforcement interaction, an analysis of some additional failure modes was performed. The external modes of overturning and sliding were investigated, while internal modes relating to pull-out failure and tensile failure of the reinforcement were not considered.

This analysis was completed using two additional wall models, which were simplified from the full model to decrease computation time and to achieve the desired failure mode.

The first model used to investigate localized failure utilized an elastic material for the foundation soil beneath the MSE wall. This would prevent failure of the foundation material and force failure to occur within the wall itself. The modulus values needed to be adjusted from the soil hardening modulus values used for each soil type in the original model (E_{ref}, E_{oed}, E_{ur}) to a single E_{50} value for each soil type. Recall that the elastic soil model will NOT take into consideration the stress history of the soil, adjusting the modulus to account for confinement and stress history. The E_{50} values were adjusted so that roughly the same settlement of the wall occurred as had been achieved during the actual construction of the wall.

Once the foundation materials were adjusted accordingly, the wall was constructed instantaneously, ignoring undrained behavior. The ultimate settlement of the wall was checked to ensure that roughly the same settlement was present. At this point, a Phi-C reduction was used to determine the factor of safety (given in Plaxis as ΣMsf) for the wall and the failure mode.

Figure 37 shows a plot of the factor of safety versus deflection for a point within the wall backfill. The deflections are extreme, as is expected from a Phi-C reduction using the Plaxis software. Both the case investigating the wall at full height WITH

surcharge and the case of the wall at final height are given in the figure. As seen, there is no significant difference between the two cases, with a factor of safety against overturning being about 2.1 for both cases.

Figure 38 shows a plot of the deformed mesh following the Phi-C reduction. With the entire foundation being an elastic material, the failure mode is forced to be an overturning failure, as seen in the figure.

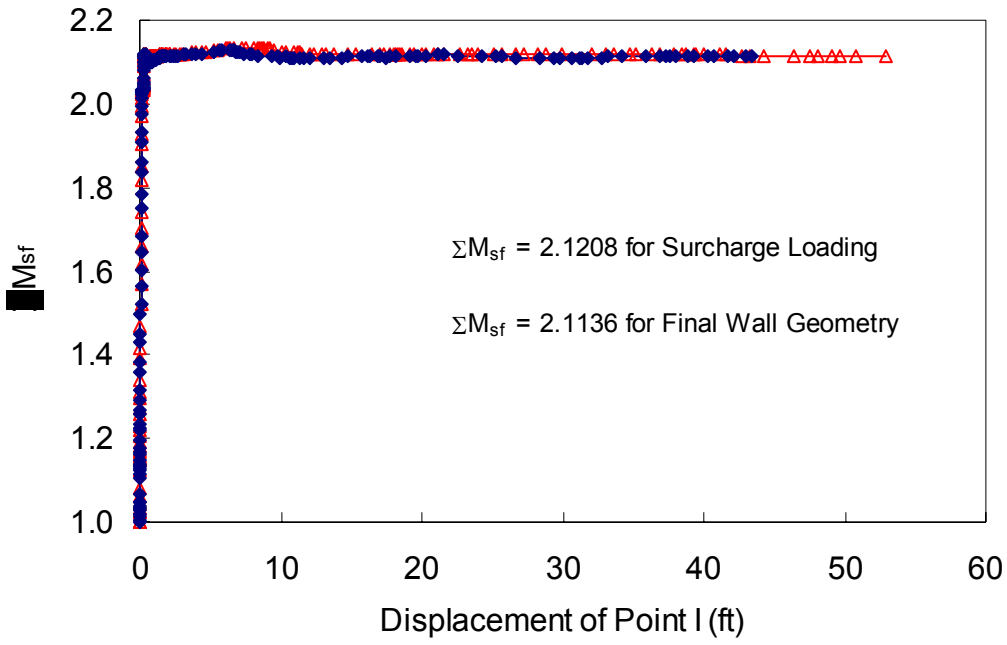

Figure 37 Factor of Safety versus Deflection of Point within Wall Backfill for Overturning Failure

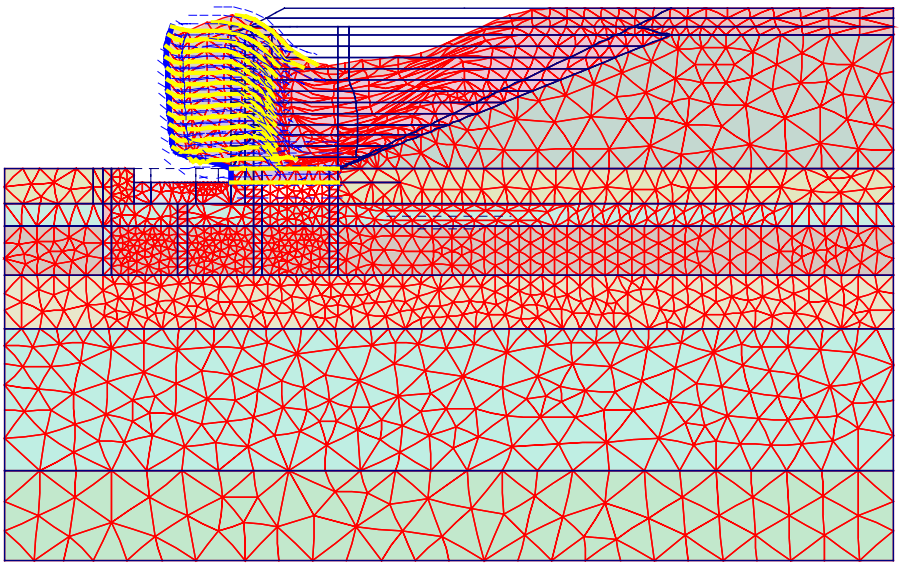

Figure 38 Deformed Mesh Following Phi-C Reduction for Overturning Failure

Next, the failure mode of sliding was investigated. To allow sliding to occur, the granular fill beneath the wall and the clay soil above the water table were again given the hardening soil properties assigned for the full model. The remaining foundation materials were left with the elastic properties as given in the overturning investigation. A loading sequence identical to the full model investigation was performed, such that the granular fill and the upper clay would have identical modulus values as the full wall model. At this point, the entire wall was constructed instantaneously, again ignoring undrained behavior, and a Phi-C reduction was performed to determine the factor of safety. As before, factors of safety were calculated for both the wall with surcharge applied and the wall at final height. A plot of the factor of safety versus deflection for a point within the wall backfill is given in Figure 39, with a plot of the deformed mesh following the Phi-C reduction given in Figure 40. Again, the factor of safety is essentially identical in comparing the wall with surcharge to the final wall geometry.

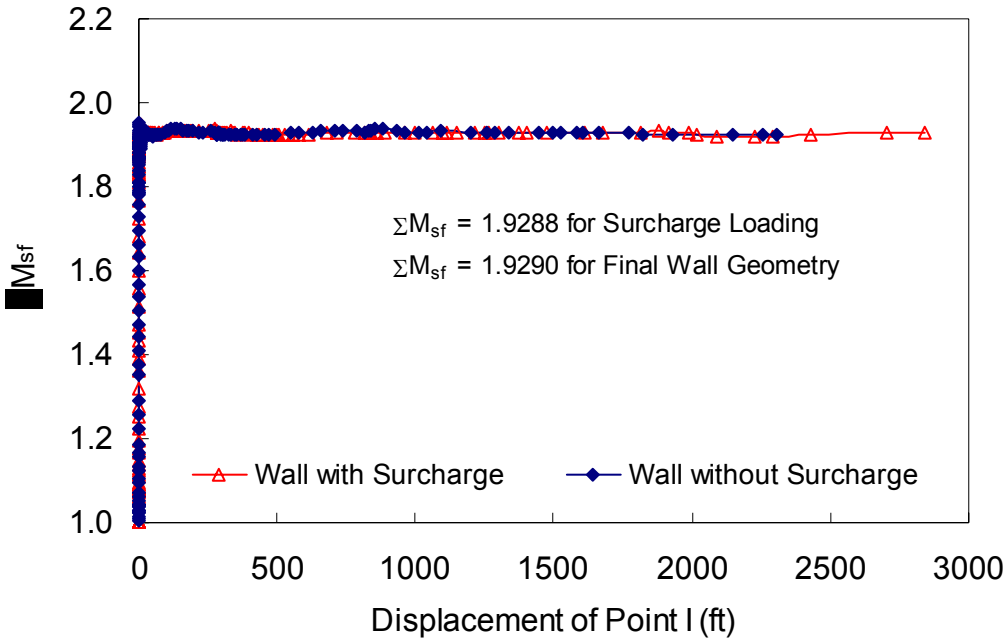

Figure 39 Factor of Safety versus Deflection of Point within Wall Backfill for Sliding Failure

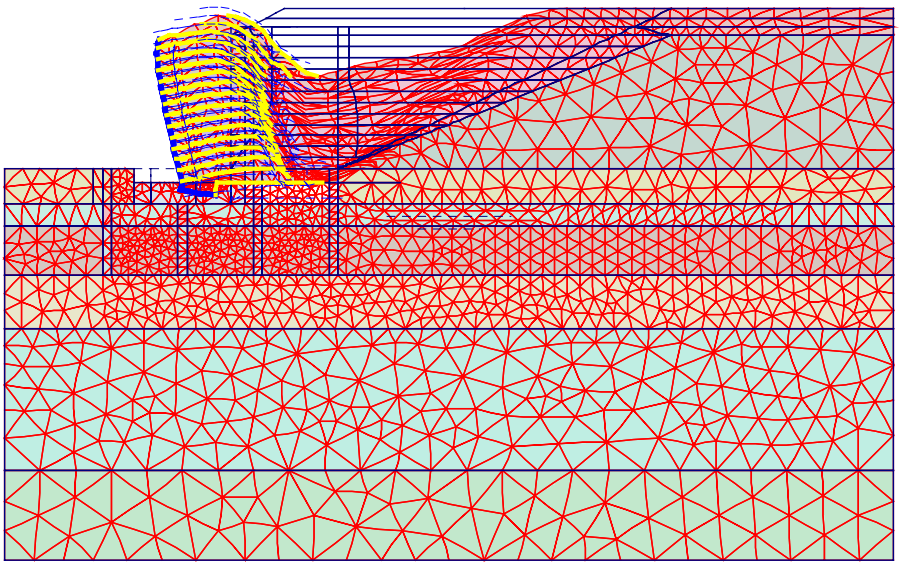

Figure 40 Deformed Mesh Following Phi-C Reduction for Sliding Failure

As seen in comparing Figure 37 to Figure 39, it appears that the factor of safety is lower for the sliding mode of failure (1.93) than for the overturning mode of failure (2.12). However, both failure mechanisms have a higher factor of safety than that found for the wall when investigating the external stability (1.67), such that the external stability appears to be the controlling method of failure.

8.0 Conclusions

This report presents the results of a finite element model of the mechanically stabilized earth (MSE) wall located on I-15 at 3600 South in Salt Lake City, Utah. The model was created and calibrated using data collected at the construction site during and after construction of the wall, as well as using the results of extensive laboratory testing on samples collected at the site. Such a model is a powerful tool in understanding the behavior of a tall MSE wall on a compressible foundation.

This analytical model includes a number of soil models to represent the range of soils in the foundation of the wall, as well as additional soil models to represent the fill material used for the original I-15 embankment and the new material used to construct the MSE wall. Trench drains, with adjusted soil permeabilities, were used to represent the prefabricated vertical drains (PVDs) used at the site. The bar mat reinforcement used to construct the wall was also modeled, with special consideration as to the effects of soil-reinforcement interaction.

The analytical model was calibrated to match the measured long-term horizontal and vertical deflections at the wall site. Once this was accomplished, the effective permeability of the foundation soil was adjusted and the construction sequence approximated in order to match the time settlement behavior of the wall. When the model was considered to accurately represent the MSE wall for both the long- and short-term behavior, a stability analysis was performed at various stages of construction to observe the global stability of the wall throughout the construction process and in the years following construction. For the model following the staged construction of the

wall, the factor or safety for the original embankment was 2.03. This value increased slightly as the wall was built, since initially the wall acted as a berm, forcing the failure surface up the embankment. However, once the wall was approximately halfway constructed, the failure surface was forced into the foundation material, and the factor of safety decreased to a minimum value of 1.47 at the application of the surcharge load, then increased with consolidation to a value of 1.69 for the long-term factor of safety for the MSE wall at final grade. A minimum factor of safety of 1.16 was calculated for instantaneous construction of the wall, which increased with consolidation to a value nearly identical to the long-term value obtained from the staged construction.

As determined during the global stability analysis, the predicted failure surface has a V-shape, with total movement being downward and away from the original embankment in the backfill material and the foundation material beneath the wall backfill, and with total movement being upward and away from the wall in the foundation material outside the wall footprint. It is noteworthy that such a failure surface might not be predicted using some automated traditional slope stability analyses, where a circular or spiral failure surface is typically used to compute a factor of safety. Slope stability software packages that allow for manually specified failure surface could better approximate such a failure mechanism, assuming such a surface was anticipated by the user. For this case, it appears that a traditional slope stability approach might not be conservative, especially if the stability analysis required a circular or spiral failure surface. This is a key reason for using a finite element program to perform slope stability (or other stability) evaluations instead of the more traditional software packages that may be limited to circular or spiral failure surfaces.

The effects of pore pressure dissipation during construction can be evaluated, and were taken into account during the stability analyses and in calibrating the time-settlement behavior. The effects of excess pore pressure were significant. Substantial excess pore pressures developed during the construction process, and dissipated with time. However, the pore pressures that developed were much less than those that would occur if an immediate, undrained construction had occurred. Thus, an undrained strength approach would be quite conservative, while a drained strength approach would be

unconservative. Using a soil model that accounts for the generation and dissipation of pore pressures and accounts for those excess pore pressures in performing stability analyses is of the utmost importance.

The ability to model the interaction between the soil and the reinforcement is somewhat limited, due to the limitations in the Plaxis software. However, a model was developed that overestimates the tension in the reinforcement in the lower portion of the wall while underestimating the tension in the upper portion of the wall. With this limited and simplified model of the soil-reinforcement interaction, an analysis of some additional failure modes was performed. The external modes of overturning and sliding were investigated, while internal modes relating to pull-out failure and tensile failure of the reinforcement were not considered. These analyses resulted in a factor of safety for sliding of approximately 1.9 and a factor of safety for overturning of approximately 2.1.

9.0 Implementation

Plaxis can be a very useful tool for the Utah Department of Transportation. It is a powerful tool for evaluating excavations, sloped embankment, and mechanically stabilized earth (MSE) walls. Plaxis can be used both for preliminary analysis of potential design strategies, and for detailed design.

For preliminary analyses, the basic input parameters may be estimated based upon data from similar sites and empirical relationships. Parametric studies may be performed to determine which of these parameters are the most critical to the behavior of the system. Preliminary analyses can be used to compare different design concepts, identify critical failure modes, determine if PVD's will be required to meet the construction schedule, determine if staged construction will be required for short-term stability, and to determine the potential effects of the project on adjacent structures and utilities.

Plaxis is also a powerful tool for detailed project design. More detailed data on subsurface conditions are required for this level of analysis. Parametric studies from the preliminary analysis will have identified which parameters are most critical to the

performance of the system. This information will enable the designer to develop a field and laboratory investigation program to obtain the critical data. When the investigation shows variability or other uncertainty in critical parameters, ranges of parameters can be used in the model to evaluate the possible behavior of the system.

Once an appropriate model or models have been developed, there are a number of evaluations that can be performed. The strength and stability of a structure can be evaluated over time, especially during the consolidation of the structure, where the influence of pore pressure generation can significantly affect the stability. Different construction sequences can be evaluated. Deformations that may occur during or after construction may be evaluated. Possible failure mechanisms can be investigated. The model can be used to determine the most economic or most efficient method of mitigating stability problems. The effects of settlement on adjacent structures or buried utilities can easily be determined.

Plaxis can provide safe, economic, and efficient designs for various geotechnical structures. The fact that Plaxis models pore-pressure dissipation during and after construction means that it provides a safe alternative to overly conservative undrained analyses. The use of Plaxis in design will allow for easy comparisons of many different design strategies which should allow the designer to select the most cost-effective, safe design for geotechnical systems.

10.0 References

Bay, J.A., L.R. Anderson, A.S. Budge, and M.W. Goodsell. 2003. Instrumentation and installation scheme of a mechanically stabilized earth wall on I-15 with results of wall and foundation behavior. Report No. UT-03.11, Utah Department of Transportation, Salt Lake City, Utah. 353 p.

Bay, J.A., L.R. Anderson, J.C. Hagen, and A.S. Budge. 2003. Factors affecting sample disturbance in Bonneville clays. Report No. UT-03.14, Utah Department of Transportation, Salt Lake City, Utah. 249 p.

Bay, J.A., L.R. Anderson, T.M. Colocino, and A.S. Budge. 2003. Evaluation of SHANSEP parameters for soft Bonneville clays. Report No. UT-03.13, Utah Department of Transportation, Salt Lake City, Utah. 50 p.

Goodsell, M.W. 2000. Instrumentation and installation scheme on a mechanically stabilized earth wall on I-15. Unpublished MS thesis. Utah State University, Logan, Utah. 133 p.

Hagen, J.C. 2001. Factors affecting sample disturbance in Bonneville clays. Unpublished MS thesis. Utah State University, Logan, Utah. 233 p.

Plaxis: Finite Element Code for Soil and Rock Analyses, Version 7. 1998. Edited by R.B.J. Brinkgreve and P.A. Vermeer. A.A. Balkema Publishers, Rotterdam, Netherlands. Approx. 427 p.